ANL-7957
LMFBR Sodium Technology
(UC-79a)

ARGONNE NATIONAL LABORATORY
9700 South Cass Avenue
Argonne, Illinois 60439

SODIUM TECHNOLOGY QUARTERLY REPORT
April-June 1972

L. Burris	Manager, Sodium Technology Program
J. E. Draley	Asst. Manager
P. A. Nelson	Section Head, Engineering Development
F. A. Cafasso	Section Head, Chemical Development
T. F. Kassner	Group Leader, Metallurgical Development
J. M. McKee	Problem Leader, Engineering Development
C. C. McPheeters	Problem Leader, Engineering Development
R. J. Meyer	Group Leader, Analytical Development

Compiled and Edited by
G. M. Kesser

November 1972

Previous quarterly reports issued in this series:

ANL-7846	April-June 1971
ANL-7868	July-September 1971
ANL-7916	October-December 1971
ANL-7944	January-March 1972

DISCLAIMER

FOREWORD

The Sodium Technology Quarterly Report describes the current activities of the Sodium Technology Program at Argonne National Laboratory, sponsored by the Coolant Chemistry Branch of the USAEC Division of Reactor Development and Technology. In the areas of sampling and analysis and on-line monitoring of impurity elements, Argonne is involved in research and development as well as in the coordination of national efforts to meet the near-term needs of sodium technology, particularly those of FFTF. Argonne's program also includes research and development work on fission-product behavior and control, sodium chemistry, and materials-coolant compatibility. The program is a coordinated effort between two Argonne Divisions--Chemical Engineering and Materials Science--with assistance being given on specific problems by the EBR-II Project and the Idaho Facilities.

TABLE OF CONTENTS

TABLE OF CONTENTS

LIST OF FIGURES

LIST OF FIGURES

LIST OF TABLES

SODIUM TECHNOLOGY QUARTERLY REPORT
April-June 1972

ABSTRACT

The research, development, and management efforts of Argonne National Laboratory's Sodium Technology Program for the period April-June 1972 comprised activities in the following areas: (1) Design work has been started on a multipurpose sampler for use at FFTF; the sampler will provide the capability for obtaining overflow sodium samples, filtering flowing sodium for assay of particulates, and equilibrating metal specimens. (2) In the analytical standards program, efforts were continued on the preparation of RDT standards on specifications for measuring and controlling the purity of sodium and cover gas and on laboratory work related to the methods to be used for purity measurement, with emphasis on equilibration methods for determining the activities of carbon, oxygen, and hydrogen in sodium. (3) Performance-characterization tests of an improved electrochemical oxygen meter having a thoria-yttria electrolyte and a gas reference electrode have been completed; other work on meters has included testing of on-line monitors for hydrogen and leak detectors for steam generators, and testing of meter modules. (4) Work was continued on the design and fabrication of a cover-gas analysis system for separating ^{23}Ne from noble-gas fission products in cover gas; testing of a laboratory prototype of a system for monitoring the ^{135}I content of reactor primary sodium was begun; and development work was continued on an on-line diffusion meter for monitoring tritium in sodium. (5) Studies of the chemistry of liquid sodium have been directed toward evaluation of vacuum distillation as a means of determining nonmetallic impurities in sodium and investigations of oxygen-hydrogen interactions in sodium. (6) Work has continued on the program to determine the integrated effects of fast-neutron and sodium environments on the properties of stainless steel and to develop postexposure testing methods for the stainless steel specimens; in the study of carbon transfer in sodium-steel systems, a mathematical model is being developed for predicting the magnitude and rate of carbon migration in reactor sodium systems.

SUMMARY

Sodium Sampling

Multipurpose Sodium Sampler for FFTF. The Sodium Technology Program at ANL has accepted the responsibility for the design and testing of the sodium sampling facilities to be used in FFTF. Design work has been started on a multipurpose sampling system that will provide the capability for overflow sampling, archive sampling, equilibration of metal specimens, and particulate sampling. The multipurpose sampler will replace the previously planned combination of a vacuum distillation/overflow sampler and a wire

equilibration device. A large fraction of the sodium technology effort at ANL during the first half of FY 1973 will be devoted to this project.

Analytical Standards Program

Sampling and Analysis of Purchased Sodium. ANL has designed a sampling system to procure overflow samples of purchased sodium during tank-car loading operations. The sampling system operates in parallel with the existing loading system. After removal from the system, the sodium samples are protected from the atmosphere by gas-tight crimp seals.

Conformance analyses of sodium purchased by Hanford Engineering Development Laboratory (HEDL) will be performed at ANL. To minimize the number of samples required for these analyses, several of the procedures in RDT F 3-40 have been combined and are now being checked out.

Particulate Analysis. Samples of the particulate collected from the Core Components Test Loop (CCTL) and from EBR-II sodium are now under examination. Bulk analysis has shown that both systems have particulate present in the range of 1 ppb. Further characterization of the particulates has been carried out using autoradiography, ion microprobe mass analysis, and gamma spectrometry.

Uranium-Getter Method for Oxygen in Sodium. Experiments to determine the applicability of the uranium-getter method for determining oxygen in flowing sodium have continued. A recent experiment suggests that a substantial quantity of the oxygen in the Test and Evaluation Apparatus (TEA) is either adsorbed on the walls or is in solution in a form other than oxide.

Determination of Carbon Activity in Sodium. A method has been developed for measuring the chemical activity of carbon in sodium. The method is based on the equilibration of Fe-8Ni or Fe-12Mn in sodium. Equations have been derived for both Fe-8Ni and Fe-12Mn to relate the carbon activity to the carbon concentration in the tabs after equilibration.

Niobium Equilibration Method for the Determination of Oxygen Activity in Sodium. The base technology has been developed for application of niobium as a detector for measurement of oxygen activity in sodium by the equilibration method. Oxygen distribution-coefficient measurements have been conducted at 500, 550, 600, 650, 700, and 750°C. As in the V-O-Na system, high corrosion rates and changes in surface condition of the niobium wires were observed above a specific oxygen level in the sodium at each temperature. This type of behavior is attributed to an equilibrium between the metal, oxygen in sodium, and a complex oxide such as sodium niobate. Although the range of oxygen concentrations in niobium is less than expected on the basis of the $Nb_{(Osat)}$-NbO equilibrium, niobium can be used to measure the range of oxygen potentials typically encountered in reactor sodium.

Application of the Equilibration Method to the Measurement of Hydrogen Activity in Sodium. Development work has continued on investigating the feasibility of measuring hydrogen activity in sodium by the equilibration of niobium and vanadium. Recent work has been directed toward testing experimental procedures for quenching the samples after equilibration. A final report will be published when all analytical data are available.

The feasibility of using other specimen materials for determining hydrogen activity in sodium is also being investigated. On the basis of a literature review, yttrium was selected as the first material to be tested. A technique in which the yttrium specimens are encapsulated in nickel is being investigated as a means of avoiding redistribution of the hydrogen in yttrium specimens during cool-down after equilibration at 750°C. Preliminary results are described.

On-Line Impurity Monitors

Oxygen Meter Characterization. The ANL-Westinghouse program on the characterization of oxygen meter performance has been completed. The Westinghouse oxygen meter tested in this program, which has a ThO_2-Y_2O_3 electrolyte and a gas reference electrode, was found to be capable of measuring the oxygen activity in flowing sodium systems with adequate accuracy if calibrated periodically by the vanadium equilibration method. A single equilibration at the normal oxygen level of the system approximately once a month is sufficient. At 900°F, the recommended operating temperature, 95% of all oxygen meter readings will agree with that determined by vanadium equilibration within a factor of 1.2.

Operation of the oxygen meters on the Oxygen Meter Rig (OMR) is being continued to determine the life of the electrolyte tubes. None of the 11 tubes has failed as yet after 8 1/2 months of service. The reference gas in five of the meters on the OMR has been changed from air to argon-100 ppm oxygen, and a twelfth meter with a tin-tin oxide reference electrode has been added to the loop. Calibrations now in progress will show whether meter performance is improved with a lower oxygen potential at the reference electrode. One of the two oxygen-meter electrodes in the module on the Test and Evaluation Apparatus (TEA) failed during the quarter after 11 months of operation at 700-900°F.

Electrochemical oxygen meters have been used during oxygen distribution-coefficient investigations to provide additional data on oxygen concentration and interactions of oxygen with other elements in sodium. Although several types of meters have been used, emphasis was placed on cells with Na-Na_2O reference electrodes. General observations regarding the behavior of electrochemical oxygen meters, based on experience with several types of meters, are presented.

Hydrogen Meter Development. Modifications are being made on the hydrogen-meter system in the oxygen-hydrogen meter (O-H) module on the Test and Evaluation Apparatus (TEA). These modifications, which will provide for reorientation of the vacuum system and hydrogen conditioning of the nickel membrane, are expected to provide improved performance of the meter during equilibrium-mode operation at low (<0.05 ppm) hydrogen

concentrations in sodium. Similar changes will be made on the hydrogen-meter system on the O-H module at EBR-II after prooftesting of the modified system on TEA.

During hydrogen and oxygen equilibration experiments in the Recirculating Sodium Equilibration Apparatus (RSEA-2), two diffusion-type hydrogen meters were operated on the sodium apparatus. The results obtained from these meters contribute to the interpretation of the equilibration data. The probe from one hydrogen meter was submerged in the high-temperature equilibration vessel on the sodium apparatus and was operated at the equilibration temperature, typically 500-750°C. The other meter was installed "on-line" and was operated at 400 or 450°C. The gauge pressures for the two meters were recorded as a function of cold-trap temperature after extended loop operation at constant system conditions. Good agreement between the output of the two meters was obtained.

Meter Modules. A prototype specimen basket designed to fit in the carbon meter-equilibration (C-E) module has been successfully used to equilibrate sheet and wire specimens in the OMR. The basket has a greater capacity than the original wire holder and provides complete containment of the specimens. A similar basket will be fabricated for use at EBR-II. Drawings have been prepared and submitted to EBR-II for comment.

ANL has agreed to supply the Liquid Metal Engineering Center (LMEC) with three low-cost specimen-equilibration devices plus a single instrumentation console serving all three.

Detectors for Leaks in Steam Generators. Two leak detectors were supplied by ANL to LMEC for use on the Sodium Components Test Installation (SCTI). Both units were installed by LMEC and are performing as designed after minor modifications to attain better temperature control. Performance tests were conducted on both leak detectors by lowering the membrane temperature by 100°F and observing the change in ion-pump current. Both units indicated a need for baking out and this bake-out procedure was conducted. After bake-out, both meters indicated a hydrogen level of $\sim$0.03 ppm in the SCTI.

When water was added to the steam generator, a substantial diffusion of hydrogen from the water to the sodium occurred, and the concentration rose to $\sim$0.2 ppm in the sodium. The source of hydrogen is thought to be water-side corrosion of the steam-generator tubes; decomposition of hydrazine in the feed water is also a possible source.

Apparatus for Monitoring and Purifying Sodium (AMPS). Construction of AMPS, the facility that will be used to develop methods for tritium monitoring and control, is nearly complete. Leak testing of the sodium containment system is in progress. Wiring and thermal insulation will be completed in July. Designs of the tritium probes for use in sodium and cover gas are nearing completion.

Fission Product and Cover Gas Technology

Development of FEDAL Methods for FFTF. Two methods for detecting fuel-element cladding failures are under development: analysis of the cover gas for noble-gas fission products and analysis of the primary sodium for ^{135}I.

Three specifications have been written for three subsystems of the cover-gas analysis system: (1) Specification HWS 1920 for the cover-gas sampling subsystem, (2) Specification HWS 1917A for the failure-detection subsystem, and (3) Specification HWS 1917B for the failure characterization subsystem. Standard RDT C 14-3, "Gamma-Ray Spectrometer-Computer System," with revisions, was approved by RDT and has been issued as a tentative standard.

Installation of Prototype Detection Systems on EBR-II. Recent price quotations from suppliers for fabrication of valves and level indicators built to applicable RDT standards have indicated that the cost of installation of the sodium sparger on EBR-II cannot be accommodated in the budget for FY 1973. The installation has, therefore, been deferred, and only laboratory tests will be performed during FY 1973. Fabrication of the laboratory test apparatus is continuing.

The cover-gas analysis system to be installed at EBR-II will be essentially identical to the system designed for FFTF. A prototype of this system is being built for testing at ANL-Illinois. Some of the valves and flowmeters for this prototype system have been ordered.

The system for analysis of sodium for ^{135}I by sparging will require an efficient vapor trap to separate entrained sodium vapor and mist from the sparge-gas stream. Tests were performed to determine the quantities of sodium entrained in a gas stream as a function of sodium temperature, gas flow rate, and gas composition (helium, argon, and helium-argon mixtures). In general, it was found that argon cover gas entrained $\sim 10^3$ times as much sodium aerosol as did helium at low (100 cm^3/min) flows and ~ 40 times as much at high (1000 cm^3/min) flows. These results suggest that aerosol formation may be due to gas-turbulence forces as well as buoyancy forces.

On-Line Tritium Monitor. Development of a tritium monitor is continuing. Calculations of tritium and hydrogen diffusion rates through a nickel membrane have been made. Nickel has been chosen as the diffusion membrane for various reasons, including its greater resistance than iron to nitriding in reducing (hydrogen) atmospheres. Two membranes have been designed: one for use in the specimen equilibration module and one for use in the Westinghouse oxygen-meter housing. The expected HT pressures and corresponding disintegration rates have been calculated for each probe design and the results of these calculations are presented.

In preparation for installation of a tritium monitor on AMPS, several tests have been conducted with the tritium detector to determine optimum operating conditions. These tests have included determinations of the optimum concentration of quench gas (methane) in the gas in the ionization chamber, the effect of ionization-chamber volume, and the effect of hydrogen

concentration in the sweep-gas on the count rate. The results of these tests are reported.

Sodium Chemistry

Vacuum distillation of sodium followed by analysis of the residue is being investigated as a method for the analysis of impurities in sodium, including oxygen. Oxygen is determined indirectly by analyzing the residue for sodium and calculating the oxygen content on the assumption that the residue consists only of sodium oxide. Thus, a correction must be made for any sodium-bearing impurities remaining in the residue. In recent work, the effect of cyanide on the determination of oxygen was investigated. Results showed that ∿50% of the added cyanide remained in the residue after distillation. This finding indicates that the presence of cyanide in sodium samples analyzed for "oxygen" will require analysis of the residue for cyanide and application of an appropriate correction.

The potential of the distillation method for the analysis of sulfur was also explored. Several tests were conducted in which known amounts of sulfur were added to the sodium before distillation. Recoveries of sulfur were only ∿50-70%. Hence, the method does not appear promising for the determination of sulfur in sodium.

Experimental work has been concluded on the study of the behavior of hydroxide in liquid sodium. Recent work has been concerned with the effect of hydrogen on hydroxide decomposition. Analysis of the data is in progress.

Materials-Coolant Interactions and Mechanical Property Evaluations

Development of Test-Specimen Characterization Methods and Procedures. An investigation of phase instabilities in Types 316 and 304 stainless steels as a function of time, temperature, degree of cold work, and carbon and nitrogen content of the materials is in progress to obtain a direct knowledge of the capabilities of various specimen-characterization methods and to provide base-line microstructural information on thermal aging effects in the materials used in this program. Additional information has been obtained on material from a small heat exchanger constructed from Type 304 stainless steel as to the nonmetallic element composition, the types of phases present, their relative amounts, and the microhardness. The experimental procedures and analysis methods that are being developed for correlating the composition and thermal history of austenitic stainless steels with the microstructures will be further used in the characterization of specimens prior to and after mechanical testing in a high-temperature sodium environment.

Development of Specimen-Exposure Facilities and Postexposure Mechanical-Property Testing Capability. Five Satec uniaxial creep machines are now operational in either an air or vacuum environment. Tests are being conducted in vacuum on Type 316 stainless steel specimens fabricated from heat V87210 for comparison with reported creep data on this material to evaluate the performance of these testing machines. An argon gas system has been designed for this equipment so that creep tests can also be performed in an inert-gas environment.

Studies of Carbon Transfer in Sodium-Steel Systems. A mathematical model is being developed to predict the magnitude and rate of carbon migration in FFTF and LMFBR systems under conditions in which temperature gradients and materials of different composition are present in the system. These effects can then be related to mechanical-property changes in the materials. The first step in the development of such a model is the formulation of rate equations for the carburization and decarburization of austenitic stainless steels. The mathematical formalism for internal oxidation was modified to represent the carburization process more closely; however, the diffusion equations became more complex and a closed-form analytical solution could not be obtained even for simple boundary and initial conditions. Therefore, a numerical solution to the problem was obtained using a computer.

The thermodynamic and kinetic input data used in the diffusion relations are those that express the driving force for carbon migration in the material in terms of the carbon-activity differences and the tracer or self-diffusion coefficient in austenite, rather than changes in the total carbon concentration and the apparent or effective diffusion coefficient. Both types of information can be used to generate carbon diffusion profiles in austenitic stainless steels: the former approach is applicable to a wide range of temperatures and carbon levels in the materials, whereas the latter is restricted to specific conditions because of limited data for the dependence of the effective diffusion coefficient on both temperature and carbon level in the steel.

Carburization-decarburization profiles for Type 304 stainless steel were obtained as a function of time, temperature, and the carbon concentration in sodium. The manner in which the diffusion behavior is influenced by incorporating both experimental and extrapolated carbon activity-concentration data for the material into the computer solution of the diffusion equations was also determined. Predictions on the carburization-decarburization behavior will be compared with measured carbon-diffusion profiles in the steel at several exposure times, temperatures, and carbon levels in sodium to establish the validity of the results.

I. SODIUM SAMPLING
(J. T. Holmes)

Multipurpose Sodium Sampler for FFTF. The Sodium Technology Program of ANL has accepted the responsibility for the design and testing of the sodium sampling facilities to be used in FFTF. The device originally designed for this use is called the Vacuum Distillation/Overflow Sampler (VD/OS). Comparison of the VD/OS design with the latest set of desired capabilities and space and funding limitations revealed some significant discrepancies. The single, rather small sampling cell of the FFTF is intended to provide overflow sampling, archive sampling, equilibration of metal specimens, and particulate sampling for five separate sodium systems, with some redundancy desired. The VD/OS was designed primarily for vacuum distillation of overflow samples in situ and cannot easily be modified to provide flexibility of function. For example, the sample cup is part of the pressure boundary, and samples for different analyses require different cup materials. Thus, considerable difficulty would be encountered in meeting the Class I ASME Code requirements with this design.

Review of these considerations led to the development at ANL of a new, multipurpose sampler design. The pressure boundary in this design is a vertical length of 2-in. stainless steel pipe with remotely or manually operable closures located in a relatively cool zone at the top of the sampler. Different internal devices are mounted inside this pipe to accomplish specimen equilibration, overflow sampling, or sodium filtration. This unit would also replace the Wire Equilibration Device (WED); therefore, there would be two units on each sodium system, providing valuable redundancy. ANL believes that the multipurpose sampler will save both money and space and provide more flexibility of function than the previously planned combination of the WED and the VD/OS.

A large fraction of the sodium technology effort at ANL will be devoted to this project during the first half of FY 1973 to meet the stringent FFTF schedule requirements.

II. ANALYTICAL STANDARDS PROGRAM
(R. J. Meyer)

A. Administrative Activities (F. A. Cafasso, R. J. Meyer)

1. RDT Standards

Argonne National Laboratory has the responsibility for generating all RDT standards related to purity specifications for sodium and gases used in reactors or other sodium systems. These documents will specify (1) acceptable impurity levels for the purchase of sodium and cover gas and for the operation of sodium and cover-gas systems and (2) the sampling and analytical methods for monitoring all impurities and for demonstrating that certain impurities (for which methods of control exist) are at or below the acceptable level.

The current status of each of the standards presently being prepared on sodium and cover-gas purity is given in Table II-1.

TABLE II-1. Status of RDT Standards

Standard Designation	Title	Status	Next Action
RDT A 1-5	Purity Specifications for Operating Sodium Systems	Revision in progress	Submit for review (August 1972)
RDT F 3-40	Interim Methods for the Analysis of Sodium and Cover Gas	Submitted for approval (May 1972)	Revise as necessary and issue (October 1972)
RDT M 13-1 Rev. 1[a]	Reactor Grade Sodium--Purchase Specifications	Approved	Issue (October 1972)
RDT M 14-1	Sodium Cover Gas--Purchase Specifications	Approved	Issue (July 1972)

[a]This document will supersede RDT M 13-1T.

2. Sampling of Purchased Sodium
(F. A. Cafasso, R. J. Meyer, H. S. Edwards, J. W. Allen)

The specifications given in RDT M 13-1, Rev. 1, "Reactor Grade Sodium--Purchase Specifications," call for the collection of three overflow samples from each lot of sodium during tank car loading: one sample of ∿10 g taken in quartz and two samples of ∿50 g taken in tantalum. (The analyses to be performed on these samples are discussed

in the following section.) Three such samples will be used to establish the purity of sodium currently being manufactured by E. I. duPont de Nemours to fill an order for HEDL. Because duPont does not presently have the capability of collecting overflow samples, ANL has been requested to assist duPont in upgrading their sampling capabilities.

To date, ANL has designed an overflow sampling system (Fig. II-1) that is compatible with the operational restraints imposed by the tank-car loading operation. The sampling system will be connected in parallel with the existing tank-car loading system, and samples will be taken according to the following procedure: The sampling system is evacuated to about -23 in. of Hg (the pressure in the tank car) and flow is established by opening the valves to the sampler and throttling the valve on the main loading system. After ∿15 min, flow to the sampler is stopped by proper manipulation of the valves, and the excess sodium is discharged from the sampler with inert-gas pressure. The samples are then cooled and the copper tubing at each end of the sampler is crimped to provide a gas-tight seal.

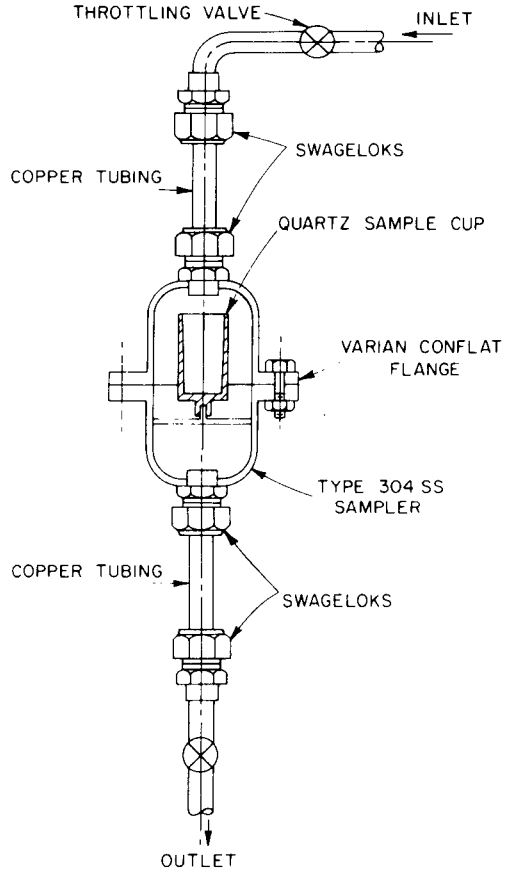

Fig. II-1

Design of System for Sampling Purchased Sodium

The sealed samples will be shipped to ANL where conformance analyses will be performed. Materials for this sampling system are on order and are scheduled for delivery early in July.

B. Laboratory Activities

1. Procedures for Analysis of Purchased Sodium
(F. A. Cafasso, R. J. Meyer, H. S. Edwards, F. R. Lawless)

As discussed in the preceding section, the purity of purchased sodium will be determined from analysis of three overflow samples. The first of these samples, ∿10 g of sodium contained in quartz, will be used to determine the carbon content of the sodium by the oxyacidic flux method. The second sample, ∿50 g of sodium contained in tantalum, will be used to determine boron, calcium, chloride, lithium, and uranium. These analyses are performed on the residue remaining after distillation of the sodium. The third sample, ∿50 g of sodium in tantalum, will be used to determine total purity, potassium, and sulfur. Methods for all the analyses except sulfur are currently included in RDT F 3-40, "Interim Methods for the Analysis of Sodium and Cover Gas;" the method for sulfur was recently developed by C. C. Miles of ANL-West.

The requirement of performing multiple analyses on the two 50-g samples has necessitated that several of the procedures in RDT F 3-40 be combined. These combined procedures have now been written and are in the process of being checked out.

2. Analysis for Particulates in Sodium
(M. D. Adams)

a. Analysis of Sodium from the Core Components Test Loop (CCTL)

A second sample of particulate material has been collected from CCTL by means of a filter (pressed-and-sintered Type 304 stainless steel) of the all-welded design previously used (ANL-7944, p. 26). In the first test, a quantitative measure of the total amount of particulate could not be obtained because of a small hole that developed in a welded region. The second particulate sample collected from CCTL was subjected to bulk analysis (total concentration), autoradiography, microscopic analysis, and examination of selected particles or agglomerates by the ion microprobe mass analyzer. The results are summarized below:

1. The amount of particulate (∿9 mg) collected represents a concentration of 2.6 ppb, based on the total sodium content of CCTL (1000 gal).

2. Autoradiography did not indicate the presence of uranium. Uranium was of interest because fuel elements containing uranium were being tested in CCTL.

3. A large number of particles of Al_2O_3 up to 0.10 mm in diameter were collected. These particles were identified both microscopically and by ion microprobe analysis. Most of these particles were

rounded and worn, which indicates that they had been in the sodium for a long period of time.

4. Alumina-silica materials related to mullite ($Al_6Si_2O_{13}$) were identified. Ion microprobe analysis showed that calcium and magnesium were also associated with these particles.

5. Compounds of the formula MN_2O_4 (where M is Fe or Mg and N is Al, Cr, or Fe) were present.

6. Metallic particles varied greatly in composition. Alpha iron, pure nickel, nickel-chromium mixtures, and stainless steel particles were found.

b. Analysis of Sodium from EBR-II

Examination of the particulate from a second filtration of EBR-II primary sodium is in progress. (Results of the first filtration were presented in ANL-7916, pp. 39-45.) In the second test, 2060 gallons were passed through a 10-μm stainless steel filter at 0.5 gpm and 600°F. The weight of particles collected was 9.9 mg; this corresponds to a particulate concentration of 1.4 ppb in the sodium.

The size distribution of the particles was determined by microscopic counting of representative areas of membrane filters on which the particles were deposited after ultrasonic cleaning of the stainless steel filter element. The size-distribution data are summarized in Table II-2.

Prior to ultrasonic cleaning, the stainless steel filter element was examined by gamma spectrometry to determine the radioactive species present. The membrane filters used to collect particulates after ultrasonic cleaning were also examined. Analysis of the gamma-spectrometric data has not yet been completed. However, preliminary results show that,

TABLE II-2. Size Distribution of Particles from EBR-II Primary Sodium

Particle Size, μm	Number of Particles
<5	$\sim 1.5 \times 10^6$
5-10	$\sim 9 \times 10^4$
10-20	$\sim 2 \times 10^4$
>20	$\sim 1 \times 10^4$

as in the previous filtration of EBR-II sodium, manganese-54 remained attached almost quantitatively to the stainless steel filter, whereas cesium-137 was removed almost completely by ultrasonic cleaning.

3. Uranium-Getter Method for Oxygen in Sodium
(H. S. Edwards, R. C. Haglund, P. J. Mack)

The applicability of the uranium-getter method for the determination of oxygen levels in flowing sodium is being investigated. The most recent experiment, which was conducted in the Test and Evaluation Apparatus (TEA), was aimed at determining how precisely uranium tabs would remove a known quantity of oxygen that had just been added, in the form of Na_2O, to a sodium system of low oxygen concentration.

With the cold trap at 210°C, successive tab insertions were made to getter the whole system, including the cold trap, until the oxygen level (as indicated by oxygen-activity meters on the system) was $\sim$0.15 ppm. This is a practical lower limit for gettering because opening the system--to remove tabs, for example--is likely to introduce $\sim$0.1 ppm of oxygen. Next, sodium flow to the cold trap was shut off and a stainless steel mesh "tea bag" containing 505 mg of Na_2O (purity, $\geq$95%) was inserted into the main reservoir of the loop. After a 30-hr delay, the oxygen meter readings (taken at 480°C) indicated the start of oxide dissolution. When the meter response had stabilized at an indicated oxygen level of 4.7 ppm, two uranium tabs were exposed to the flowing sodium at 520°C. After about 30 hr, the oxygen meters again indicated an oxygen level of $\sim$0.15 ppm; but, unavoidably, the tabs were left in place for another 40 hr. At the time of tab removal, the oxygen meters indicated $\sim$0.1 ppm oxygen.

The total weight gain of the two tabs was 179.9 mg. On the basis of the amount of sodium in the system, this weight gain is equivalent to a removal of 21.2 ppm oxygen from the system. This finding was surprising since the oxygen meters had indicated an oxygen level of 4.7 ppm when the tabs were inserted. Moreover, the addition of Na_2O should have raised the oxygen level to only 15.4 ppm. Although the reason for these discrepancies has not been determined, it has been concluded tentatively that a substantial quantity of oxygen in TEA either is adsorbed on the walls or is in solution in a form other than oxide; for example, sodium carbonate or sodium formate could be produced by the reaction of dissolved oxygen with the free carbon known to be circulating in the sodium in TEA. Experiments to substantiate this conclusion are now under consideration.

4. Measurement of Carbon Activity in Sodium
(M. F. Roche, J. W. Allen, R. J. Meyer)

A method of measuring the chemical activity of carbon in sodium has been developed. The method is based on the equilibrium distribution of carbon between sodium and a tab of Fe-8Ni or Fe-12Mn immersed in the sodium. With graphite chosen as the standard state, the chemical activity of carbon in the tab and in sodium is the same at equilibrium. The carbon activity of the metal, and consequently that of the sodium, can then be derived from carbon analysis of the metal tab and from the established relationship between carbon concentration and carbon activity in the tab

alloy. This method is analogous to the vanadium-wire method that is used to measure the oxygen activity in sodium.[1] At a given activity, the equilibrium carbon content of Fe-12Mn is about three times that of Fe-8Ni; thus Fe-12Mn is a more useful monitor in systems having lower activities.

The primary use of the tab-equilibration method will be in determining the chemical activity of carbon in sodium systems. These measurements and measurements of carbon activity *vs* carbon concentration for sodium-system materials of construction, such as Type 304 stainless steel, are needed for predicting the direction and rate of carbon transport in sodium systems.[2] If carbon meters are present in the sodium system, the tab-equilibration method would also serve to evaluate and calibrate the on-line meters.

a. Chemical Activity of Carbon in Fe-8Ni and Fe-12Mn

Carbon activity measurements in our experiments have been based on an extrapolation to 700°C of an equation of Bodsworth *et al.*[3] for relating carbon concentration to carbon activity in Fe-Ni-C alloys. (The simultaneous equilibration of Fe-8Ni and Fe-12Mn tabs at 700°C in sodium enabled us to derive an equation relating carbon activity to carbon concentration in Fe-12Mn that is based directly on the equation for Fe-8Ni.) The equation of Bodsworth *et al.* was derived, however, from data obtained in the temperature range from 850 to 1050°C. We therefore expected that the extrapolation of his equation to 700°C would involve some error.

An experiment conducted in sodium saturated with carbon has now shown that the carbon activity at 700°C is a factor of 1.20 higher than estimates based on Bodsworth's equation. In the experiment, 500 mg of Na_2C_2 was added to sodium contained in a 1000-cm^3 alumina crucible, and the sodium temperature was raised to 700°C. Tabs of Fe-8Ni, Ni, and Fe were suspended in the sodium on nickel wires, and the sodium was stirred throughout the 3-day equilibration by means of a nickel stirrer. The results of carbon analyses on these tabs, after electropolishing to remove surface carbon, are given in Table II-3. The results for Ni and

TABLE II-3. Carbon Analyses of Tabs from Ceramic-Pot Experiments at 700°C

Tab Material	Carbon, ppm
Fe-8Ni	3985, 3841, 3900
Ni	572, 512
Fe	144, 132

[1]D. L. Smith, Nucl. Technol. 11, 115 (1970); D. L. Smith and R. H. Lee, ANL-7891 (January 1972).
[2]K. Natesan and T. F. Kassner, J. Nucl. Mater. 37, 223 (1970).
[3]C. Bodsworth *et al.*, Trans. Met. Soc. AIME 242, 1135 (1968).

Fe are in good agreement with recent evaluations of measurements of the solubility of graphite in these materials at 700°C. The recommended values are 520 ppm for the solubility of graphite in nickel,[4] and 127 ppm for the solubility of graphite in iron.[5] Thus, we concluded that the experiment was conducted in sodium saturated with carbon. The average value obtained for the solubility of graphite in Fe-8Ni at 700°C in our experiment is 3909 ppm, a value 700 ppm lower than that estimated from the equation of Bodsworth et al. Adjustment of Bodsworth's equation to reflect this measured solubility leads to the following equation for the activity of carbon in Fe-8Ni at 700°C:

$$a_c = \frac{\text{ppm C}}{4234 - 0.083 \text{ ppm C}} \qquad (1)$$

This equation is in good agreement with the data of Natesan et al.[6] on carbon activity vs. carbon concentration for carbon activities in Fe-8Ni ranging from 0 to 0.66. The corresponding equation for the activity of carbon in Fe-12Mn at 700°C is

$$a_c = \frac{\text{ppm C}}{13480 - 0.264 \text{ ppm C}} \qquad (2)$$

Equation 2 was derived from Eq. 1 and data relating the carbon concentration in Fe-8Ni to that in Fe-12Mn over carbon activities ranging from 0.002 to 0.3 (ANL-7944, p. 16, Fig. I-1).

b. Decarburization of Type 304 Stainless Steel Tabs in the Oxygen Meter Rig (OMR)

In a recent experiment, Type 304 stainless steel tabs of 3-mil thickness, equilibrated in flowing sodium in the Oxygen Meter Rig (OMR) at 700°C for a period of three days, were decarburized from their initial carbon concentration of 340 ppm to a concentration of 30 ppm. Simultaneously equilibrated Fe-12Mn tabs indicated a carbon activity of 3.3×10^{-3}, in good agreement with previous determinations of carbon activity in the OMR based on Fe-8Ni and Fe-12Mn equilibrations (ANL-7944, pp. 14-16). The decarburization behavior of the Type 304 stainless steel tabs in the OMR is significantly different from the behavior of Type 304 stainless steel tabs equilibrated at the same carbon activity (again as indicated by Fe-8Ni and Fe-12Mn tabs) in well-stirred 700°C sodium held in a Type 304 stainless steel pot (ANL-7944, pp. 16-18). In the pot-type experiment, considerably less decarburization of the stainless steel tabs occurred: their carbon concentrations decreased from 340 ppm to only ∿200-300 ppm. A factor of ten difference thus exists between the pot measurements and loop measurements. Additional experiments are in progress in an effort to determine the cause of this difference.

---

[4]T. Wada et al., Met. Trans. 2, 2199 (1971).
[5]J. Chipman, Met. Trans. 3, 55 (1972).
[6]K. Natesan et al., Sodium Technology Quarterly Report, January-March 1972, ANL-7944, p. 53, Fig. V-5 (in press).

5. Niobium Equilibration Method for the Determination of Oxygen Activity in Sodium (D. L. Smith)

Detailed procedures and distribution-coefficient data for application of the equilibration method to the measurement of oxygen activity in liquid sodium have been developed,[1] and the feasibility of applying the equilibration method to the measurement of carbon,[7-9] nitrogen,[10] and hydrogen[11] activities in liquid sodium has been demonstrated. The base technology is also being developed for the application of niobium as a detector for measurement of oxygen activity in sodium by the equilibration method.

The primary advantage of niobium as a detector compared with vanadium is the capability of measuring oxygen concentrations in the range of interest, i.e., $\leq$20 ppm oxygen in sodium, with lower equilibration temperatures. The procedures used are similar to those described for the vanadium-wire equilibration method.[1] Niobium wires of 0.50-mm diameter are recommended because of the lower distribution coefficient and hence the lower oxygen concentration in niobium than in vanadium. Increased accuracy in the oxygen analysis of the niobium by inert-gas fusion techniques is obtained with the larger wires.

The minimum equilibration times for oxygen in niobium as a function of temperature are given in Table II-4 for 0.25-mm-dia and 0.50-mm-dia wire.

Distribution-coefficient measurements have been conducted at 500, 550, 600, 650, 700, and 750°C. The sodium systems used for the V-O-Na distribution-coefficient measurements were also used in these tests. When appropriate, vanadium wires have been exposed simultaneously as an additional check on the oxygen concentration in sodium. Both inert-gas fusion techniques and internal friction measurements have been used in the oxygen analyses of the niobium. The internal friction measurements are more sensitive for the small sample size, particularly at the lower oxygen concentrations. The distribution-coefficient results obtained to date at 650 and 750°C are given in Fig. II-2. At 650°C the oxygen concentration in niobium is dependent on that in sodium at levels up to 30 ppm

---

[7] K. Natesan and T. F. Kassner, "Monitoring and Measurement of Carbon Activities in Sodium Systems," submitted for publication in Nucl. Technol.

[8] Sodium Technology Quarterly Report, January-March 1971, ANL-7817, pp. 69-72 (July 1971).

[9] Sodium Technology Quarterly Report, January-March 1972, ANL-7944, pp. 14-17 (in press).

[10] Reactor Development Program Progress Report, January 1968, ANL-7419, pp. 103-105 (January 1968).

[11] Sodium Technology Quarterly Report, October-December 1971, ANL-7916, pp. 45-47 (May 1972).

TABLE II-4. Minimum Time Required to Equilibrate Oxygen in Niobium Wires Exposed to Liquid Sodium

Equilibration Temperature, °C	Equilibration Time,[a] hr	
	0.25-mm dia	0.50-mm dia
550	22	88
600	9	36
650	4	15
700	2	7
750	1	4

[a]Based on diffusivity data of Powers and Doyle, J. Appl. Phys. 10(4), 514-524 (1959).

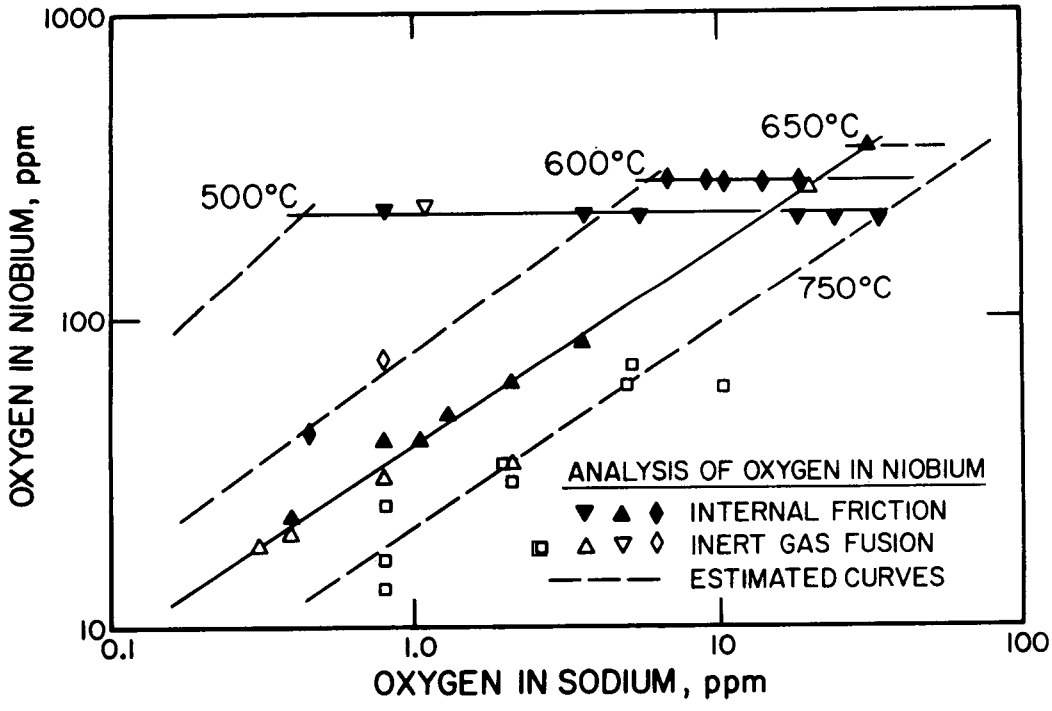

Fig. II-2. Measured Oxygen Concentrations in Niobium after Exposure to Sodium of Various Oxygen Concentrations. Neg. No. MSD-57614

oxygen in sodium. As in the V-O-Na system, the distribution coefficient ($K_A = N_{O\_Nb}/N_{O\_Na}$) for this system is also temperature dependent, i.e., it increases with a decrease in temperature. Since all of the analyses have not been completed for the samples exposed at the other temperatures, the additional results will be included in a final report which will be submitted for publication.

Above certain oxygen levels in sodium at each temperature, high corrosion rates and changes in surface condition of the niobium wires were observed after exposure to sodium. After removal of any surface films and surface contamination, the wires from these tests were analyzed for oxygen. Results obtained at 500 and 600°C (Fig. II-2) show that constant oxygen concentration in niobium were obtained under these conditions. Similar behavior was also observed in the V-O-Na system.[12] The intersection of curves of this type with the concentration-dependent curves determines the maximum oxygen concentration in sodium that can be measured by the equilibration method at each temperature.

Gaseous oxidation experiments with niobium in a Sieverts' apparatus were conducted to investigate the substantial differences between the maximum oxygen concentrations in niobium from Fig. II-2 and the oxygen-solubility data previously considered to be the most reliable.[13] Internal friction measurements on samples from these tests indicated that oxygen was in solution in the niobium at concentrations as high as 1000 ppm at 500°C. This value is slightly above the reported solubility curve[13] and much greater than the apparent solubility values obtained from the horizontal curves in Fig. II-2. The oxygen concentrations of 220 and 280 ppm at 500 and 600°C, respectively, are attributed to an equilibrium between the metal, oxygen in sodium, and a complex oxide, probably sodium niobate. Because of nonadherency of this oxide phase, as indicated by the high corrosion rate, sufficient material has not been obtained for positive identification. Although the range of oxygen concentrations in niobium is less than expected on the basis of the $Nb_{(Osat)}$-NbO equilibrium, niobium can be used to measure the range of oxygen potentials typically encountered in reactor sodium.

6. Application of the Equilibration Method to the Measurement of Hydrogen Activity in Liquid Sodium

a. Equilibration Studies with Niobium and Vanadium (D. L. Smith)

The objective of this work is to determine the feasibility of using an equilibration method to measure the hydrogen activity in liquid sodium. In conjunction with the oxygen distribution-coefficient studies, niobium and vanadium wires have been exposed to sodium at temperatures from 500 to 750°C for hydrogen analyses. Earlier experiments (ANL-7916, pp. 45-47) indicated a dependence of the hydrogen concentration in the wires on the cold-trap temperature of the sodium. In these tests, the equilibration samples were withdrawn from the sodium into a gas lock

[12] D. L. Smith, Met. Trans. 2, 579-583 (1971).
[13] T. F. Kassner, D. L. Smith, ANL-7335 (1967).

above the liquid level. The gas lock was immediately isolated and the wires were allowed to cool in the sealed chamber. Although generally reproducible hydrogen concentrations in the detectors were obtained, the values were considerably higher than those calculated from available thermodynamic data. Several variations in the experimental procedure have been tested in an attempt to determine if changes in hydrogen concentration during quenching from the equilibration temperature were responsible for the unexpectedly high hydrogen concentrations. These included varying the quenching rate, quenching without isolating the chamber from the cover gas, and encapsulating the detector wires in nickel capsules. The final tests in this series have been completed. Since a number of samples are still awaiting analysis, the results will be included in a final report.

b. Equilibration Studies with Yttrium (D. R. Vissers)

Development work on an equilibration method for determining hydrogen activity in sodium has been extended to include a search for other specimen materials. It is hoped that the method will also be applicable to the determination of tritium in sodium. A literature review has suggested that yttrium might be a suitable specimen material. The distribution coefficient for hydrogen between yttrium and sodium is significantly higher (by a factor of perhaps 500-1000) than that between niobium (or vanadium) and sodium.

Analysis of diffusion effects has indicated that at 750°C (the temperature at which vanadium specimens are equilibrated for determining oxygen activity) significant redistribution of hydrogen may occur during cool-down of the yttrium specimens. This problem can be avoided by displacing the sodium with inert gas at 750°C or by encapsulating the yttrium in a material such as nickel. Encapsulation in nickel would reduce the rate of hydrogen diffusion into and out of the yttrium and would also avoid possible problems resulting from interactions of the specimen material with sodium and/or its other impurities.

Preliminary tests of the encapsulation technique were conducted by exposing encapsulated yttrium specimens to flowing sodium at 750°C. Exposures were carried out at several different hydrogen levels in sodium, in the range from 0.05 to 0.85 ppm. Although the results of these first tests were not conclusive, the encapsulation technique appears to be a promising means of avoiding the problem of redistribution of hydrogen upon cool-down.

Further studies will be conducted to evaluate (1) the encapsulation technique and (2) the use of yttrium and other candidate materials for determining hydrogen activity in sodium.

III. ON-LINE IMPURITY MONITORS
(J. M. McKee)

Argonne National Laboratory is coordinating, as well as participating in, a national program for development, testing, and establishing commercial availability of impurity meters for use in LMFBR sodium systems. The meters being developed and characterized in this program are monitors for oxygen, carbon, and hydrogen impurities in sodium; the hydrogen meter is also being tested as a leak detector for steam generators. Standardized modules are being developed to provide (1) flow and temperature control for the meters and (2) a means for obtaining independent impurity measurements by equilibration of metal specimens.

A. Oxygen-Meter Characterization

1. ANL-Westinghouse Joint Test Program
(D. R. Vissers, J. M. McKee, L. J. Marek, L. G. Bartholme)

The ANL-Westinghouse oxygen-meter characterization program has been completed. The goal of this program was to provide a statistically significant measure of the calibration stability of the Westinghouse oxygen meters, which are fabricated with ThO_2-Y_2O_3 electrolytes and gas reference electrodes. This goal has been achieved. Twenty oxygen meters were tested in this program: 10 at Westinghouse Advanced Reactor Division (WARD) and 10 at ANL in the Oxygen Meter Rig (OMR). All 20 meters were operated at 700°F to evaluate their calibration stability. In addition, the stability of the 10 ANL meters was evaluated at 900°F. The oxygen meters were calibrated at eight oxygen levels in sodium by the vanadium equilibration method, which is used to determine the oxygen activity in sodium. In some instances, oxygen analyses by the amalgamation method were also performed on samples of sodium.

The principal conclusions drawn from the tests are as follows:

(1) The commercially available meter tested in this program can provide a continuous measure of the oxygen activity in reactor sodium systems with adequate accuracy if it is calibrated periodically by the vanadium equilibration method.

(2) The meter emf, which varies linearly with the logarithm of the oxygen activity in sodium, can be represented by the equation

$$\text{Meter emf (volts)} = K_1 - K_2 \log O \text{ (ppm)} \qquad (1)$$

The slope (K_2) of the calibration curve, although less than the theoretical, is consistent enough that a single value can be used for all meters at a given temperature with minimal error. The observed values of K_2 are 0.048 ± 0.002 and 0.065 ± 0.001 volts per decade in oxygen activity at 700 and 900°F, respectively.

(3) The intercept (K_1) of the calibration curve is also less than the theoretical value and is subject to drift, especially during the first month or two of operation. The value for K_1 can readily be redetermined by a single vanadium equilibration at the normal oxygen level of the system.

(4) If the meters are recalibrated monthly, the indicated oxygen level will agree (95% of the time) with that determined by the vanadium equilibration method within a factor of 1.6 at 700°F and within a factor of 1.2 at 900°F, the recommended operating temperature. The actual stability of the meter is better than these factors indicate because the value of K_1 includes the errors (estimated at ±10%) in determining oxygen in sodium by the vanadium equilibration method.

(5) The meter emf is insensitive to the small variations in sodium temperature normally encountered. However, variations in the temperature of the cooling fins on the meter housing do affect the emf significantly. It may be possible to substantially reduce this undesirable effect by immersing the electrolyte tube farther into the sodium stream, below the sodium outlet nozzle on the housing.

(6) There is, as yet, no evidence that the life of the electrolyte tube is shorter at 900 than at 700°F.

(7) Oxygen meters should probably be installed in pairs on large sodium systems. Under these conditions, if one electrolyte tube should fail, it could be replaced at the next convenient time, and monitoring of the oxygen activity of the system could continue with the second meter. The redundancy would also help to distinguish between meter drift and small fluctuations in the oxygen activity of the sodium.

(8) The precision of determining oxygen in sodium by vanadium equilibration is estimated to be about ±10 to 20%.

(9) As expected, sampling and analysis for oxygen by the amalgamation method is of no value for determining oxygen activity in sodium at the low levels typical of reactor coolant systems.

(10) Performance testing of two meters operating in EBR-II primary sodium has shown no short-term effects of radiation from ^{24}Na, to date, on the behavior of the meters.

A paper summarizing the oxygen-meter characterization program at ANL and WARD, entitled "Calibration Stability of Oxygen Meters for LMFBR Sodium Systems," will be presented at the 65th Annual AIChE Meeting in New York (November 1972).

Testing of the oxygen meters on the OMR is continuing, but at a reduced level of effort, with the primary objective of determining the life of the improved thoria-yttria electrolyte tubes. Eleven electrolyte tubes[1] on OMR have operated for 8 1/2 months (six months at 700°F, 2 1/2 months at 900°F) as of June 30, 1972, with no failures. A few failures have occurred among similar tubes tested on other sodium systems at ANL-Illinois, EBR-II, and Westinghouse. The limited data available to date

---

[1]An eleventh meter, with a thoria-yttria electrolyte tube in a United Nuclear Corporation oxygen-meter housing, was also operated at ANL during the calibration stability tests.

suggest that tube life may be affected less by sodium temperature (in the range from 700 to 900°F) than by the rate and extent of temperature changes.

Two changes have recently been made to explore the effect of lower oxygen potential at the reference electrode on meter performance. Firstly, the reference gas in Meters OM-1 through -5 was changed from air to argon containing 100 ppm oxygen. The gas is continuously refreshed by a slow bleed which flows through the five electrodes in parallel and exits to the air through a bubble counter filled with silicone oil. (The dry air in Meters OM-6 through -11 is similarly refreshed.) Secondly, an oxygen meter containing a tin-tin oxide reference electrode in place of the gas-platinum reference was installed in housing OM-12 in the OMR. Vanadium equilibrations are being performed at several oxygen levels to indicate whether any improvement in meter stability is achieved by either of these changes.

The emfs of the meters operating with a reference gas of argon-100 ppm oxygen average 76 mV below the theoretical value of 1 ppm oxygen in sodium vs. 163 mV below theoretical for the air-reference meters. Apparently, the reduced oxygen potential at the reference electrode produced a significant reduction in electronic conductance of the solid electrolyte. The meter with the tin-tin oxide electrode has a higher sensitivity than the standard meters, and its emf appeared to be quite stable after a single day of operation. Tests made prior to startup showed that the meter can be cycled through the freezing point of tin repeatedly without cracking the electrolyte tube. The temperature coefficient of the tin-tin oxide meter is positive and several times higher than that of the standard meters ($\sim$0.3 mV/°F as compared with -0.09 mV/°F for the standard meters at 900°F and 2 ppm oxygen).

2. Oxygen-Meter Performance on Other Facilities

a. Radioactive Sodium Chemistry Loop (RSCL) at EBR-II
(J. T. Holmes)

As of May 19, 1972, the two oxygen meters operating in the oxygen-hydrogen meter (O-H) module of the RSCL at EBR-II had accumulated 3565 and 3131 hr, respectively. The meters have been operated at about 700°F and have continued to show considerable drift in their voltage outputs. The meters were shut down on May 19 to perform calibration and preventive maintenance work on the instrument systems for the module and the RSCL. The oxygen meters are expected to be back in service in early July.

b. Test and Evaluation Apparatus (TEA)
(V. M. Kolba and P. J. Mack)

During April 1972, the electrode assembly of Oxygen Meter O-1 failed after a total of 8266 hr of operation. Meter O-2 continued in operation and as of June 30 had accumulated a total operating time of 9346 hr. The operating times at various temperatures are shown below:

Module Meter Number	Westinghouse Meter Number	HEDL Tube No.	Time at Temp., hr 700°F	800°F	900°F	Total Time, hr
0-1	II-E-2	73-1-2	3432	2818	2016	8266
0-2	II-E-1	72-2-1	3264	2482	3600	9346

Temperature coefficient tests conducted early in April showed that, prior to failure of the electrode, Meter 0-1 had a rather large negative coefficient (-0.125 to -0.240 mV/°F), whereas Meter 0-2 had a positive coefficient, ~0.061 mV/°F. A large negative temperature coefficient, approaching -1 mV/°F, is often indicative of imminent failure of the cell.[2]

c. Recirculating Sodium Equilibration Apparatus No. 2 (RSEA-2) (D. L. Smith)

Electrochemical oxygen meters have been used during the investigations of oxygen distribution coefficients (see Section II.B.5) to provide additional data on the oxygen concentration and interactions of oxygen with other elements in sodium. Although several types of meters have been used, emphasis was placed on cells with Na-Na_2O reference electrodes. This type of cell possesses several fundamental advantages for studies involving solutions of oxygen in sodium. These include: (1) elimination of calculational errors because of uncertainties in free energies of formation of other reference oxides, i.e., the reference is the same at both electrodes; (2) gross reductions in oxygen-activity gradients across the electrolyte which exist in other commonly used oxygen meters, thus tending to minimize undesirable electronic conductivity effects in the electrolyte; (3) lower cell emfs, which minimize current leakage; (4) liquid references at both electrodes, which result in good electrode-electrolyte contact and thus reduce contact resistance; and (5) fast response to temperature changes in the cell because the reference electrode is liquid.

The primary question in the use of electrochemical cells with Na-Na_2O reference electrodes has been concern over compatibility of the electrolyte with the oxygen-saturated sodium. Experience with cells constructed with electrolyte tubes (ThO_2-15 wt % Y_2O_3) of the type used in United Nuclear Corporation (UNC) meters has been reported previously.[3] These studies indicated stable cell operation for periods of several months. Two additional meters with Na-Na_2O reference electrodes have been operated simultaneously on RSEA-2. One of these meters, 3N, is of the same construction as the previously operated meters, i.e., a UNC-type housing with a ThO_2-15 wt % Y_2O_3 electrolyte tube. The second meter, WN, was constructed with a Westinghouse-type housing and the high purity ThO_2-7.5 wt % Y_2O_3 electrolyte tube (tube 49-3-3 made by HEDL). Figure

[2]WNICD-OM001, Instruction Manual, Westinghouse Liquid-Metal Oxygen Meter, Model LM-II (December 1970).

[3]D. L. Smith, Nucl. Technol. 11, 115-119 (1971); D. L. Smith, R. H. Lee, ANL-7891 (January 1972).

III-1 is a plot of the response of these meters (at 352°C) as a function of oxygen concentration in sodium determined from the oxygen solubility at the cold-trap temperature.[3] Vanadium-wire equilibrations were used to confirm these values at oxygen concentrations in sodium below 15 ppm. Both meters indicate a depletion of oxygen in the cold trap above 30 ppm, i.e., the cell voltages do not decrease with increasing cold-trap temperature above this level. These cells have been in operation for approximately three months. In general, the data points are within 4 mV of the curves and no significant drift in cell emf with time has been observed with either of these meters. An effect, which has been attributed to trapping of gas in the annulus of the oxygen meter housing (ANL-7846, pp. 9-13), has also been observed during recent meter operation. Voltage variations, which are recoverable by oscillating the sodium flowrate, are believed to be the major cause of scatter in the data given in Fig. III-1. This trapping and subsequent release of gas into the sodium was also observed by periodic fluctuations in flowmeter response and by small temperature changes at various locations in the loop.

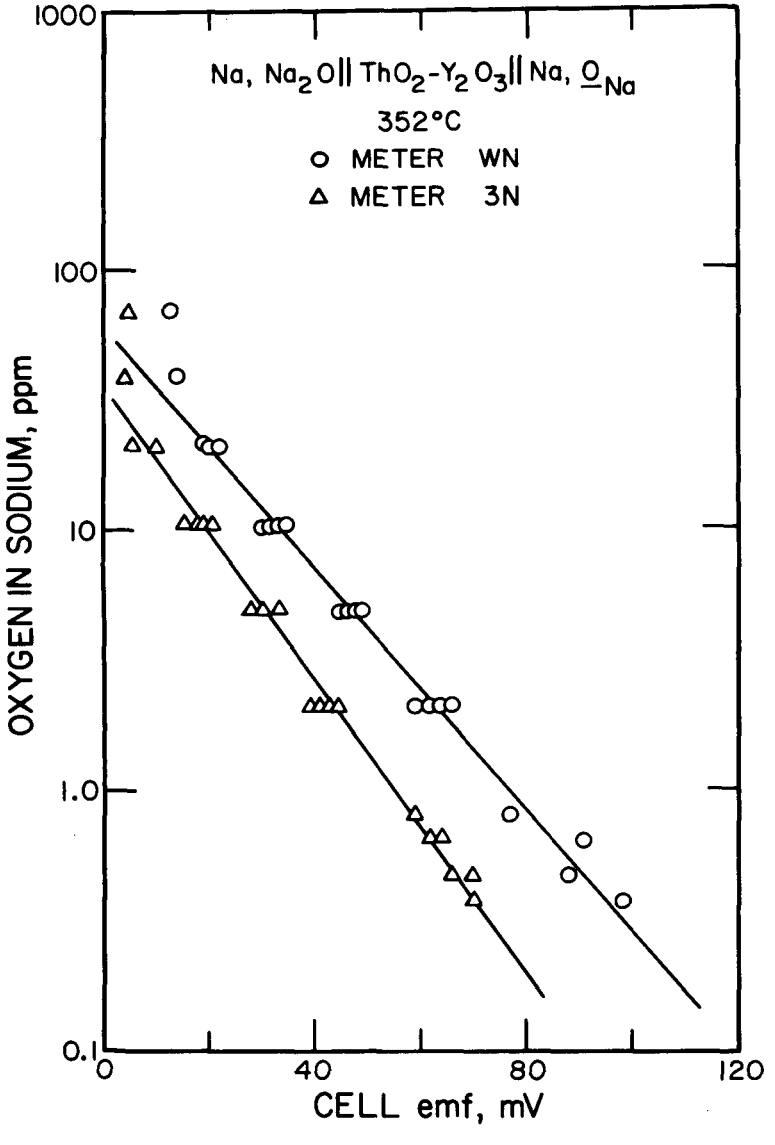

Fig. III-1

Cell Emf as a Function of Oxygen Concentration in Sodium for Two Types of Electrochemical Cells with Na-Na_2O Reference Electrodes. Neg. No. MSD-57612

The reciprocal slope of the curve for Meter 3N (∿35 mV/decade) is in good agreement with previous results from cells with Na-Na_2O reference electrodes as well as with values obtained from UNC-type meters,[3] which have similar electrolyte tubes and Cu-Cu_2O reference electrodes. The experimental slopes from all of these meters are considerably lower than the theoretical value of 62 mV/decade at the operating temperature.

The cell emf of Meter 3N is somewhat lower than the initial curve obtained previously for Meter 2N. However, this curve is in good agreement with the curve obtained for Meter 2N after hydrogen was added to the sodium. As will be discussed in Section B.2, below, hydrogen meter results indicated that in this apparatus (RSEA-2) the hydrogen content of the sodium is high, whereas Meter 2N was initially operated under low-hydrogen conditions. The null voltage intercept, which should indicate the saturation value of oxygen in sodium, was considerably lower than the reported solubility[3] value at the cell temperature.

Meter WN with the smaller diameter, high-purity electrolyte tube gave cell emfs somewhat higher than Meter 3N (Fig. III-1). The reciprocal slope of the curve for Meter WN, 43 mV/decade, is significantly greater than that for Meter 3N. However, this value is in good agreement with that reported previously (ANL-7916, pp. 17-18), 47 mV/decade, for a Westinghouse-type meter equipped with a similar electrolyte tube and operated at 400°C on the same sodium apparatus. The small difference in slopes obtained for these two meters is, in part, due to the lower operating temperature of Meter WN. The null voltage intercept of Meter WN also indicated a lower oxygen solubility in sodium, which is tentatively attributed to hydrogen effects. These observations are not as readily apparent from data obtained with the commercial meters.

After long periods of stable loop operation, the simultaneous responses of both oxygen and hydrogen meters have been recorded immediately after bypassing the cold trap. Significant changes in the meter readings have been observed under certain conditions. Final interpretation of these results is awaiting the completion of analyses of equilibration samples used to independently monitor the impurity levels in sodium after bypassing the cold trap.

The following general observations regarding the behavior of electrochemical oxygen meters are based on experience with several types of meters:

1) The slopes of curves (mV/decade in oxygen concentration) from all meters were significantly less than those calculated on the basis of ideal cell behavior.

2) Meters utilizing similar electrolyte tubes but different reference electrodes gave response curves with approximately the same slope. However, meters utilizing the same reference electrode with a different type of electrolyte tube produced curves with measurably different slopes. Present data are not sufficient to determine whether this effect is due to electrolyte purity, Y_2O_3 content of the electrolyte, or structure of the electrolyte material.

3) The presence of significant amounts of hydrogen in the sodium tended to reduce the emf of the meters without measurably affecting the slopes of the response curves. This hydrogen effect was observed with both types of electrolyte materials and occurred independently of the reference electrode. The reduced emfs are tentatively attributed to conductivity effects in the electrolyte; however, hydrogen interactions with the electrolyte at the sodium side of the cell may also be a contributing factor.

B. Hydrogen-Meter Performance

1. Hydrogen Meter on TEA
(V. M. Kolba, J. T. Holmes, P. J. Mack)

The hydrogen meter in the O-H module in the RSCL of EBR-II continued in operation in the dynamic mode until May 19, 1972, when the module was shut down. Planned modification of the meter are expected to improve the performance of the hydrogen meter in the equilibrium mode at low (<0.05 ppm) hydrogen concentrations in sodium. The modifications will first be made on the hydrogen-meter system of the O-H module on TEA. The changes, which will provide for reorientation of the vacuum system and hydrogen conditioning of the nickel membrane, involve (1) placing the ionization gauge closer to the membrane, (2) reducing the volume of the system when the meter is operated in the equilibrium mode, and (3) reducing the number of flanged connections between the membrane and the vacuum valve to a minimum. Drawings for these modifications have been made, and fabrication of the piping for the unit on TEA has been started.

If these modifications result in improved meter performance, the hydrogen-meter system in the O-H module at EBR-II will be modified during a future shutdown when the module can be removed for the required cutting, welding, and relocation of components and supports. Modifications similar to those described above have also been made on the hydrogen-meter system of the O-H module to be used on the Apparatus for Monitoring and Purifying Sodium (see Section III.E, below).

2. Hydrogen Meters on RSEA-2 (D. L. Smith)

Two diffusion-type hydrogen meters have been operated on the sodium apparatus used for the hydrogen equilibration experiments with niobium and vanadium (Section II.B.6). The results obtained from these meters contribute to the interpretation of the equilibration data. The probe from one hydrogen meter was submerged in the high-temperature equilibration vessel on the sodium apparatus and operated at the equilibration temperature, typically 500-750°C. The other meter was installed "on-line" and was operated at 400 or 450°C. Figure III-2 is a plot of the measured gauge pressure as a function of cold-trap temperature recorded for the two meters after extended loop operation at constant system conditions. The data indicate good agreement between the two meters. However, the pressure obtained from the on-line meter was dependent on the time at which it was recorded, since the pressure continued to drift. The response curve of this meter was similar to that reported for the hydrogen meter

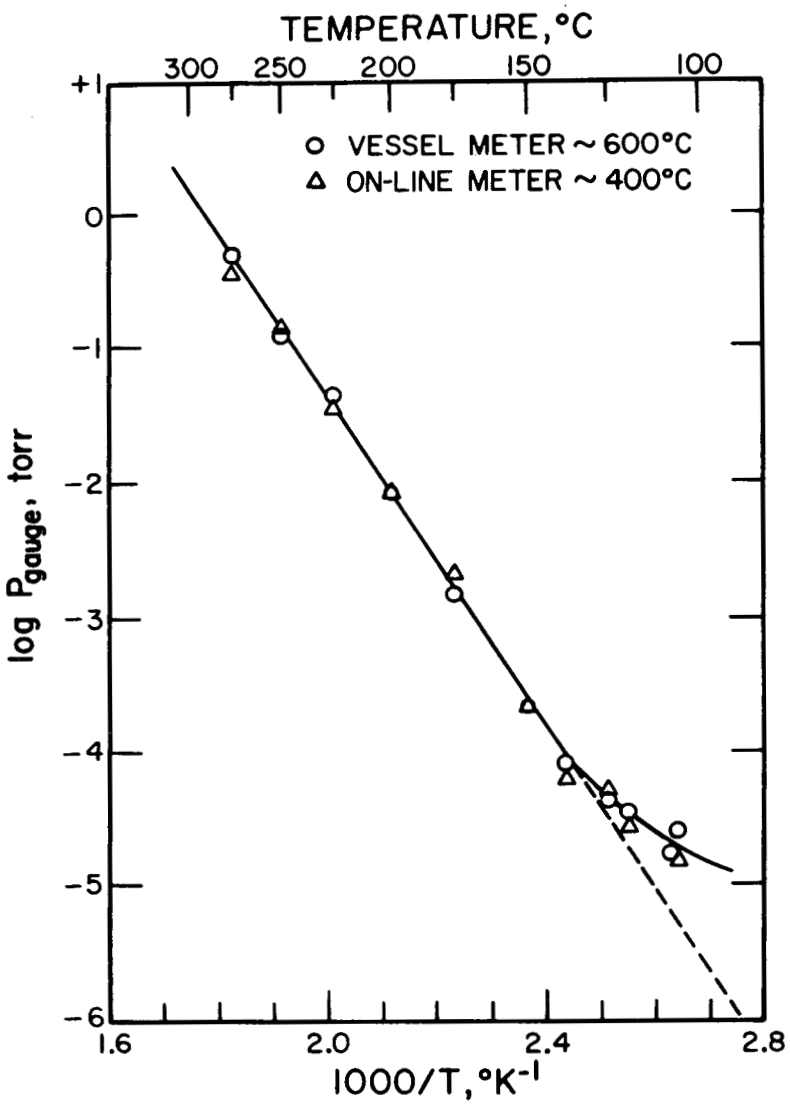

Fig. III-2

Gauge Pressure for Two Hydrogen Meters as a Function of Sodium Cold-Trap Temperature.
Neg. No. MSD-57835

operated at 700°F on TEA.[4] The values given in the figures for the on-line meter were recorded 90 min after closing the valve. In contrast, the vessel meter maintained constant pressure for periods exceeding two weeks. The stability of the vessel meter is emphasized by the fact that reproducible pressures were obtained with this meter after increasing the cold-trap temperature for a few days and then returning it to the previous lower temperature, while maintaining the meter in the equilibrium mode (valve closed). If the gauge pressures in Fig. III-2 are multiplied by a factor of 3.0 to convert to hydrogen pressure, the results are in good agreement with data reported by other investigators.[5-9]

---

[4]Sodium Technology Quarterly Report, July-December 1971, ANL-7868, p. 17 (1972).
[5]M. A. Herold, Compt Rend. 228, 686 (1949).
[6]C. C. Addison, R. J. Pulham, and R. J. Roy, J. Chem. Soc. 116-121 1965.
[7]D. W. McClure and G. D. Halsey, Jr., J. Phys. Chem. 69, 3542 (1965).
[8]S. A. Meacham, E. F. Hill, and A. A. Gordus, USAEC Report APDA-241 (1970).
[9]D. R. Vissers, J. T. Holmes, and P. A. Nelson, Trans. Amer. Nucl. Soc. 14(2), 610 (1971).

The measured pressures, which deviate from the linear curve (Fig. III-2) at the low cold-trap temperatures ($\leq$130°C), are believed to be a better indication of the true hydrogen pressure in sodium than values predicted from extrapolation of the linear curve. Evidently the rate of hydrogen diffusion through the containment vessel was sufficient to contribute measurably to the hydrogen concentration and pressure in sodium at the lower levels attainable by cold-trapping. This conclusion is supported by data obtained when the cold trap was bypassed after long periods of system operation at constant conditions. For initially low cold-trap temperatures, and hence low hydrogen pressures, the meter pressure rapidly increased to pressures typically in the 1-3 x 10^{-3} Torr range. At the high cold-trap temperatures, the meter typically dropped off to approximately this same level after bypassing the cold trap, indicating depletion of hydrogen from the sodium when hydrogen was not continuously supplied by the cold trap. Hydrogen pressures of $\sim$1 x 10^{-3} Torr, which corresponds to a cold-trap temperature of 175°C, are in reasonable agreement with the estimated atmospheric hydrogen partial pressure of $\sim$7 x 10^{-4} Torr (i.e., $\sim$1 vol ppm). Differences between predicted and measured hydrogen pressures in sodium at low cold-trap temperatures, thus, are not necessarily limitations of the hydrogen activity meter, but rather may result from inability to maintain low hydrogen concentrations in sodium.

The following two conclusions have resulted from the simultaneous operation of these two hydrogen meters on the same sodium apparatus. First, the drift in pressure encountered with the on-line meter is partially attributed to atmospheric hydrogen which diffuses through the high temperature portion of the vacuum line wall adjacent to the sodium loop. No drift was observed with the vessel meter on which the vacuum line was cooled to <50°C in the cover gas region of the vessel before it contacted the atmosphere directly. Therefore, improved operational behavior of on-line type meters should result from redesign of the probe to eliminate contact of the vacuum line with the atmosphere at high temperatures.

Second, the long-term (weeks) stability of the vessel meter combined with its relatively rapid response at the higher operating temperatures, $\geq$650°C, are attractive features for application of this meter as an equilibrium-mode hydrogen leak detector. Pressure variations resulting from cold-trap temperature fluctuations of only ±2°C were observable, even at pressures of 1-3 x 10^{-5} Torr. Operation of the leak detector in the equilibrium mode would eliminate the potential problems associated with variable pumping speeds of the ion pumps during operation of the meters in the dynamic mode.

C. Meter Modules (V. M. Kolba, J. T. Holmes, J. M. McKee, D. R. Vissers, M. A. Slawecki,[10] P. J. Mack, L. G. Bartholme, L. J. Marek)

The objective of this work is to design, prooftest, and establish commercial availability of on-line meter modules. These modules include impurity meters and the flow and temperature controls required for proper meter operation.

---

[10]Design Group, Chemical Engineering Division, ANL.

1. Oxygen-Hydrogen Meter (O-H) Modules

Two O-H modules, each containing two oxygen meters and one hydrogen meter, are currently being tested: one at ANL-Illinois on TEA and the other in radioactive primary sodium at EBR-II. A third O-H module has been installed on AMPS.

a. O-H Module, Cell B of the RSCL at EBR-II

The O-H module had operated with the meters at 700°F for a total of 3565 hr as of May 19, 1972, when it was shut down to perform calibration and preventive maintenance work on the module and the RSCL instruments. Operation is expected to be resumed in early July, and plans are being made to raise the operating temperature of the meters to 900°F. It is expected that operation at the higher temperature will improve the performance of both the oxygen and hydrogen meters.

b. O-H Module on TEA

The O-H module on TEA has been tested at sensor temperatures of 700, 800, and 900°F with an inlet sodium temperature of 700°F. The sodium in TEA has been cold-trapped at oxygen levels in the range of 0.5 to 40 ppm and hydrogen levels in the range of 0.025 to 3 ppm. Recently, a test was conducted to provide data on temperature distribution within the module for use by EBR-II. The module was operated with sodium-inlet temperatures of 500, 595, and 650°F and meter temperatures of 700 and 900°F at each inlet temperature. The temperature-distribution results have been sent to EBR-II.

2. Carbon Meter-Equilibration (C-E) Module

The C-E module contains a preheater and an isothermal zone (for a carbon-meter probe or for equilibration of metal specimens) in series with a regenerative heat exchanger, flow-control valve, and flow indicator. Three of these modules have been built at ANL: one is in use at ANL in the OMR, one is in operation at EBR-II in Cell C of the RSCL, and one has been installed on AMPS. The modules in the OMR and the RSCL are being used initially for calibrating oxygen meters by the equilibration of vanadium metal specimens. A fourth module was built at WARD and has been used for calibrating oxygen meters there. A fifth was built at HEDL and installed in the Sodium Characterization System of the Prototype Applications Loop (PAL).

Screen strainers (100-mesh) have been installed in the inlet and outlet piping of the C-E module in the RSCL at EBR-II. These strainers are being used to insure complete containment of vanadium-wire specimens within the module during equilibrations of the specimens for determination of oxygen activity of EBR-II primary sodium.

A new, basket-type specimen holder that provides complete containment of specimens within the basket has also been designed for use in this module. After prooftesting, the new specimen holder will replace the present holder and the screen strainers as well. Drawings of the new

holder have been submitted to the EBR-II Project for review. The new holder has a larger capacity and will provide the capability of equilibrating metal specimens in shapes other than wires, e.g., sheet specimens and encapsulated wires. A prototype specimen basket has been fabricated and has been used successfully in the OMR to equilibrate specimens of various shapes for the determination of oxygen, hydrogen, and carbon in sodium.

At the request of the Liquid Metal Engineering Center (LMEC), ANL will fabricate three low-cost equilibration devices (ANL-7916, p. 31) and a single instrument console serving all three. Procurement of materials and components will be started upon receipt of a purchase order from LMEC.

D. Detectors for Leaks in Steam Generators

1. Leak Detectors for LMEC-SCTI (C. C. McPheeters, V. M. Kolba, M. A. Slawecki[10])

Two hydrogen-meter leak detectors for water or steam leaks in steam generators have been supplied to LMEC for use on the Sodium Components Test Installation (SCTI) during steam-generator tests. Unit 1 was installed on the SCTI early in calendar 1972, and was started up during April, although some difficulty was encountered in initiating sodium flow.

The hydrogen concentration initially indicated by Unit 1 was 0.64 ppm. This level decreased slowly as the SCTI sodium was cold-trapped and a final level of $\sim$0.03 ppm was attained. The meter performance was checked by changing the membrane temperature by 100°F (900 to 800°F) and noting the change in ion-pump current. The observed change was less than theoretical and outside the allowable limits specified in the operating manual (±20% of theoretical). It was concluded that the vacuum system requried baking out. When the SCTI was shut down in May to install leak detector Unit 2, the vacuum system of Unit 1 was baked out at 150 to 250°C for approximately 1 week. The rate of heat-up to the baking temperature was carefully controlled to prevent the ion-pump current from exceeding 200 μA; this was necessary to avoid subsequent deterioration of pump performance.

After startup of the SCTI, both leak detectors indicated a hydrogen concentration of $\sim$0.03 ppm. The detectors were checked for proper operation by changing the membrane temperature by 100°F, and both units were within the allowable range of the theoretical change.

When water was added to the steam generator, both meters indicated a marked increase in the hydrogen level in the SCTI. The indicated hydrogen level rose to a maximum of $\sim$0.2 ppm while the steam generator was not yet to full operating temperature and began to subside after several days at full power. The principal source of the hydrogen is believed to be water-side corrosion of the low-alloy steel tubes in the steam generator. Some of the nascent hydrogen thus released diffuses through the tube wall into the sodium. Decomposition of hydrazine in the feed water is also a possible source of hydrogen.

2. Leak Detectors for EBR-II Steam Generators (J. T. Holmes)

EBR-II management and RDT have agreed that ten steam-generator leak detector modules of the ANL design be installed on the EBR-II secondary sodium system to provide continuous monitoring. A complete system design description is being prepared by EBR-II to supplement their recommendation. RDT has requested the incorporation of inlet and outlet sodium isolation valves on each module. EBR-II is assessing the feasibility of including the valves.

E. Apparatus for Monitoring and Purifying Sodium (AMPS) (J. M. McKee, D. J. Raue)

Construction of AMPS, the facility that will be used to develop methods for tritium monitoring and control (see Section IV.C), is nearing completion. An O-H module, two in-line samplers, two vapor traps, a tritium monitor (except for the probe), and a mixing tee have been fabricated and installed in AMPS. All welds have been inspected by radiography and dye-penetrant tests. Leak testing of the sodium-containment system is in progress. Wiring of the 54-kW main heaters, the electromagnetic pumps, the enclosure exhaust system, and two of the three cold-trap blowers was completed. All flowmeter and leak-detector leads, trace heaters, and thermocouples have been connected. Thermal insulation will be installed as soon as the trace heaters and thermocouples have been tested. Designs of tritium probes for use in sodium and cover gas are nearing completion.

IV. FISSION PRODUCT AND COVER GAS TECHNOLOGY
(C. C. McPheeters)

A. Development of FEDAL Methods for FFTF

Two methods for detecting and characterizing possible fuel-cladding ruptures in FFTF are under development. These methods involve analysis of the cover gas over the reactor and of the primary coolant. The systems developed from these methods will become part of the FFTF Fuel Failure Monitoring System.

1. Analysis of Cover Gas (C. C. McPheeters, N. R. Chellew, M. S. Foster,[1] R. W. Kessie,[1] R. D. Wolson)

The cover-gas analysis for detecting and characterizing fuel-element cladding ruptures involves sampling of the cover gas, separation of gases by chromatography, and analysis for the xenon and krypton isotopes of interest by gamma spectrometry. A system that utilizes this method has been designed. This system consists of three sections: (1) a cover-gas sampling subsystem that samples the cover gas, separates ^{23}Ne and ^{41}Ar from the xenon and krypton by chromatography, and retains the xenon and krypton near a Ge(Li) detector during gamma counting (this subsystem also includes a control console that operates the sampling valves and monitors and records the process variables); (2) a detector subsystem that includes a Ge(Li) detector, associated power supply, preamplifier, amplifier, liquid-nitrogen Dewar flask, three single-channel analyzers, ratemeters, recorders, and alarms; and (3) a characterization subsystem that includes a 4096-channel analyzer and a mini-computer for data analysis and process control.

Specifications have been prepared for each of these subsystems for use by Hanford Engineering Development Laboratory (HEDL) in ordering the system for installation on FFTF. Specification HWS-1920 for the cover-gas sampling subsystem was prepared using RDT Standard C 12-1, "Gas Chromatograph for Sodium Cover Gas Service." The Specifications HWS-1917A for the detection subsystem and HWS-1917B for the characterization subsystem were prepared using RDT Standard C 14-3, "Gamma-Ray Spectrometer-Computer System." Standard C 14-3 was approved, with suggested revisions, by RDT. These revisions have been made and the document has been issued as a tentative standard.

2. Analysis of Sodium by Sparging

A sparger and sparge-gas analysis system are being fabricated for laboratory testing at ANL-Illinois. The piping layout, valving, and component arrangement will simulate a conceptual system for LMFBR installation. During operation of the device, sodium is circulated through a sparging vessel (constructed of 2-in. pipe) that has an isolated gas space to prevent the sodium level from rising to flood the vessel. After a sufficient circulation time has elapsed for representative sodium sampling, the sodium-outlet valve is closed and the gas phase is vented to permit sodium to rise in the vessel until a signal from an inductive level sensor

---

[1]Computer Applications Group, Chemical Engineering Division, ANL.

closes the sodium-inlet valve. Argon sparge gas is bubbled through the sodium sample (~570 cm^3) and the effluent sparge gas is directed through an aerosol-trap system consisting of a packed vapor condenser and a high-efficiency filter. The gas then enters a sparge-gas analysis system, in which activities sparged from the sodium are monitored by gamma counting.

A small-scale (2.5 gal) pumped sodium circuit, designed to supply a controlled flow of sodium to the prototype sparger, has been constructed; a final helium leak-check has been performed on the system; thermocouples and heaters have been tested; and the apparatus is ready for filling with sodium. Current plans are to operate the sodium supply apparatus for a shakedown period of at least two weeks prior to installation of the sparger module.

B. Installation of Prototype Detection Systems on EBR-II (N. R. Chellew, C. C. Honesty, R. D. Wolson)

1. Sodium Sparger

Original plans were to install prototpyes of a sparger and sparge-gas analysis system as well as a cover-gas analysis system on EBR-II for testing. Recent price quotations from suppliers for fabrication of sparge-system components to applicable RDT standards have indicated that the cost of installation of the sodium sparger on EBR-II cannot be accommodated in the budget for FY 1973. Although installation of the cover-gas analysis system on EBR-II will proceed as planned, the installation of the sparging system has been deferred.

2. Cover-Gas Analysis System

The cover-gas analysis system to be installed at EBR-II is essentially identical to the system designed for FFTF. Current plans are to install this system in the experimental equipment building just outside the primary containment building at EBR-II. HEDL's Charged Tape Detector will be installed in the same area, and the same cover-gas sample line will provide samples to both systems.

A prototype of the cover-gas analysis system is being built for testing in the laboratory at ANL-Illinois prior to the installation at EBR-II. Design and drafting for the prototype are well under way, and most of the valves, flowmeters, and other hardware components have been purchased.

The prototype system will be tested using samples of argon containing ^{85}Kr and ^{133}Xe. The tests will determine the performance of the valves under continuous cyclic operation, the suitability of the chromatographic-column design for separation and retention of the isotopes during gamma counting, and the performance of the gamma-counting equipment.

3. Aerosol Collection

The prototype sparger and the sparger to be installed on EBR-II will require sodium aerosol traps that will remove entrained sodium vapor and aerosol from the sparge-gas streams. A series of experiments was

run to determine the amount of sodium aerosol expected to be generated at various temperatures and with different cover gases.

The test apparatus, which was located inside an argon-atmosphere drybox, consisted of a 2-in. schedule 40 stainless steel pipe 18 in. long. The pipe was filled with sodium (∿50 g) to a height of ∿3 in. The lower 4 in. of the tube was heated with a tube furnace while the pipe was oriented ∿40° from vertical so that the sodium pool and aerosol could be viewed through a Pyrex window at the top. The inlet and outlet for passing gas through the system were 1/4-in.-OD stainless steel tubes that penetrated the sides of the pipe. The inlet was positioned so that the gas entered the pipe near the top of the sodium pool and the outlet was ∿1 in. below the viewing window. The aerosol generated was collected on 37-mm Millipore filters (0.8 μm pore size) that were positioned in the exit stream.

Both helium and argon were used as the sodium cover gas at flow rates of 100 and 1000 cm^3/min; aerosol was collected at 350 and 450°C. During collection, a slight negative pressure was maintained on the back side of the filter with a vacuum pump.

With helium cover gas, little or no sodium could be seen collecting on the filter, and the gas space above the sodium appeared to be clear. With argon and a sodium temperature of 350°C, sodium could be seen collecting on the filter almost immediately and, although the sodium pool was visible, aerosol was present. At 450°C with argon, lumps of sodium collected on the filter in ∿2 min, and visibility was limited to ∿1 in. below the viewing window.

Mixtures of helium and argon (10 and 50% helium by volume) were also tested. Visual observation suggested that less aerosol was formed with these mixtures. However, subsequent analyses indicated that the amount of aerosol was approximately the same as with pure argon; apparently, only the particle size had changed.

The final series of tests was performed at 450°C by passing pure helium and pure argon through the apparatus at a flow rate of 1000 cm^3/min. An interesting observation during the argon test was that visibility down into the tube was increased at the higher flow rate, and the viewing glass did not fog up. Sodium was being collected at a greater rate, however, and apparently the exit tube was on the verge of becoming plugged.

With 1000 cm^3/min helium flow, the gas space above the sodium was visually clear, but a thin film of sodium could be seen collecting on the filter during the collection period.

The filter packs from all the tests were treated by a procedure which converts the sodium aerosol to stable sodium carbonate. The procedure[2] is based on (a) the reaction of sodium with water vapor to form sodium hydroxide and (b) the reaction of hydroxide with carbon dioxide to form carbonate. The Millipore filter packs for both samples and blanks (open

---

[2]F. J. Files, Jr., P. Himot, and M. W. First, High Capacity--High Efficiency Filters for Sodium Aerosol, NYO-841-10, Harvard Air Cleaning Laboratory, School of Public Health, Harvard University (August 1967).

on the floor of the box during the collection period) were taken into a glovebox which had an atmosphere of humid nitrogen and CO_2 (3% H_2O vapor and 2% CO_2 by volume). The filter packs were left in this environment for 16 hr. The filters were then treated with 100 ml of demineralized water for 24 hr to dissolve the carbonate.

Results of the analyses[3] are summarized in Table IV-1, where it can be seen that aerosol is generated at a greater rate in argon than in helium. Argon cover gas entrained $\sim 10^3$ times as much sodium aerosol as did helium at low (100 cm^3/min) flows and $\sim$40 times as much at high (1000 cm^3/min) flows. A 100°C temperature increase accounted for a 10- to 15-fold increase in aerosol generation rate in both gases. These results

TABLE IV-1. Results of Aerosol-Collection Tests

Cover-Gas Volume: 796 cm^3
Surface Area of Sodium: 28.8 cm^2

Cover Gas Composition	Temperature, °C	Aerosol Collected, mg/hr
Gas Flow Rate: 100 cm^3/min		
Helium	350	7×10^{-3}
Helium	350	a
Helium	450	7×10^{-2}
Helium	450	1.1×10^{-1}
Argon	350	25
Argon	350	19
Argon	450	215
Argon	450	215
50% Helium-50% Argon	350	14
50% Helium-50% Argon	350	14
50% Helium-50% Argon	450	201
50% Helium-50% Argon	450	207
10% Helium-90% Argon	350	12
10% Helium-90% Argon	350	13
10% Helium-90% Argon	450	188
10% Helium-90% Argon	450	132
Gas Flow Rate: 1000 cm^3/min		
Helium	450	34
Helium	450	34
Argon	450	1352
Argon	450	1440

[a]Not measurable

[3]Analyses performed by F. R. Lawless, Analytical Standards Laboratory.

suggest that aerosol formation may be due to a combination of gas momentum forces (turbulence) and buoyancy forces.

These tests have provided information on the quantity of aerosol that must be removed from the sparge-gas stream. In the sparger to be installed on EBR-II, argon must be used as the sparge gas. This is necessary because it is possible that sparge gas could be inadvertently introduced into the primary sodium stream and subsequently into the cover-gas system. If helium were used as the sparge gas and thus introduced into the cover gas, it would interfere with the gas-chromatographic analysis for hydrogen.

Additional tests are planned to determine the effectiveness of aserosol-trap designs for aerosol removal from the sparge-gas stream. The present design of an experimental trap for collection of sodium aerosols leaving the sparge vessel consists of a packed pipe, 1.05-in.-ID by 13 in. long. Sparge gas flowing at 1000 cm^3/min will be cooled from about 360 to 125°C in the trap before being directed into a high-efficiency aerosol filter. Mockups of the sparge vessel and vapor trap have been fabricated and tests are planned to evaluate the efficiency and drainage characteristics of the trap initially packed with 1/4-in.-dia Raschig rings.

C. On-Line Tritium Monitor (A. F. Panek, R. Kumar, P. A. Nelson)

In an LMFBR, tritium is produced by ternary fission in the fuel and by neutron activation of boron in the tetraboron carbide control rods. A large fraction of the tritium that is generated is released to the primary sodium. Plans are now being formulated for a study of tritium behavior at EBR-II as a function of operational changes possible within the constraints of EBR-II operation. A model of expected tritium behavior in EBR-II (as well as other LMFBRs) is being developed to guide the EBR-II tests. Another facet of this work is the development of an on-line tritium monitor to facilitate study of tritium behavior in loop systems and, probably, at EBR-II. Such a monitor could also be required on reactor-sodium and cover-gas systems.

The proposed monitor is based on the diffusion of tritium and hydrogen through a permeable membrane of iron or nickel, immersed in the circulating sodium. The tritium and hydrogen are then swept by an argon-hydrogen carrier gas into an ionization chamber for determination of tritium concentration.

Initial calculations on the diffusion of tritium through the membrane of the tritium monitor (ANL-7944, p. 35) were made for a probe consisting of an iron tube 0.375-in. OD by 3.5 in. long with a 0.018-in.-thick wall. For this probe, it was calculated that tritium levels in sodium typical of EBR-II and those expected at other LMFBRs would provide adequate tritium count rates in the ionization chamber.

Nickel has several advantages over iron as a diffusion membrane for this application. Firstly, nickel is not subject to nitriding in a reducing atmosphere such as that anticipated for hydrogen-containing sweep gas. Nitriding would impose a gradually increasing resistance to gas transport through the membrane. Secondly, data are available in the literature on

the transport of tritium and hydrogen through nickel. (In the earlier calculations, the permeabilities of ^{3}H and ^{1}H through iron were assumed to be equal for lack of more specific information on the diffusion of the two isotopes through iron.) In respects other than the nitriding problem, nickel is not expected to behave very differently from iron. The permeabilities of hydrogen through the two metals are similar, particularly at higher temperatures.

As discussed previously (ANL-7944), a diffusion-type tritium monitor could be operated in two different modes: an equilibrium mode and a dynamic mode. The dynamic mode is the more useful since the concentration of HT in the sweep gas leaving the probe is relatively insensitive to small variations in the hydrogen content of the sodium and the sweep gas, and is a function only of the tritium activity in sodium, the sweep-gas flow rate, and the probe temperature. Diffusion calculations have now been made for dynamic-mode operation of a tritium monitor with a nickel membrane. The data of Hawkins[4] on the solubilities of hydrogen isotopes in nickel and the data of Katz et al.[5] on the diffusivities were used to obtain the permeabilities of hydrogen and tritium through nickel. Two different probe sizes were used for the calculations. The membrane of the larger sized probe, which was designed to fit in the specimen-equilibration module housing, was considered to be a nickel tube 3.3 in. long by 0.375-in. OD with a 0.015-in.-thick wall. The smaller probe was sized to fit in a Westinghouse oxygen-meter housing, and its membrane was considered to be a nickel tube 1.26 in. long by 0.375-in. OD with a 0.015-in.-thick wall.

The results of the calculations for the larger probe operating at 750 and 930°F (typical temperatures expected in secondary and primary sodium in future LMFBRs) are shown in Table IV-2. The results obtained for the smaller probe at 900°F (the operating temperature in the standard O-H meter module) are shown in Table IV-3. The HT concentrations are expressed in the tables both as HT pressure and as tritium activity in the sweep gas.

Typical tritium concentrations at EBR-II are about 10^{15} atoms/kg Na and 2×10^{14} atoms/kg Na in the primary and secondary sodium, respectively. From Tables IV-2 and IV-3, it is evident that at the lower sweep-gas flow rates, both probes would provide adequate amounts of tritium for counting at these tritium concentrations in the sodium. Two such probes will be fabricated and prooftested on the Apparatus for Monitoring and Purifying Sodium (AMPS) (see Section III.E).

In preparation for operation of the monitor on AMPS, several laboratory experiments have been conducted to determine the appropriate mode of operation of the ionization counter. Generally, this work has included the determination of response characteristics of counting tubes of different volumes, optimum electronic operating conditions, and the testing of the effect of various carrier-gas compositions on the general behavior of the counting system.

---

[4]N. J. Hawkins, KAPL-868 (1953).
[5]L. Katz, M. Guinan, and R. J. Borg, Phys. Rev. B 4(2), 330 (1971).

TABLE IV-2. Computed Tritium Concentrations in Sweep Gas from a Diffusion Probe for Carbon Meter Housing--Dynamic Mode Operation

Membrane: Nickel tube, 0.375-in. OD by 3.3 in. long by 0.015-in.-thick wall

T_{Na}, atoms/kg Na	Temp., °F	Sweep-Gas Flowrate, ml/sec	P_{HT} from Probe, atm	Tritium Disintegration Rate, dps/ml of Sweep Gas
9×10^{14}	750	0.1	1.19×10^{-10}	5.75
		0.2	6.04×10^{-11}	2.9
		0.5	2.44×10^{-11}	1.2
		1.0	1.22×10^{-11}	0.6
	930	0.1	3.83×10^{-10}	18.5
		0.2	2.04×10^{-10}	9.9
		0.5	8.46×10^{-11}	4.1
		1.0	4.28×10^{-11}	2.1

TABLE IV-3. Computed Tritium Concentrations in Sweep Gas from a Diffusion Probe for Oxygen Meter Housing--Dynamic Mode Operation

Membrane: Nickel tube, 0.375-in. OD by 1.26 in. long by 0.015-in.-thick wall

T_{Na}, atoms/kg Na	Temp., °F	Sweep-Gas Flowrate, ml/sec	P_{HT} from Probe, atm	Tritium Disintegration rate, dps/ml of Sweep Gas
9×10^{14}	900	0.05	2.53×10^{-10}	12.2
		0.10	1.31×10^{-10}	6.35
		0.20	0.67×10^{-10}	3.24

To gain maximum sensitivity in the counting system, the ionization chambers are operated in the Geiger-Mueller region, rather than in the proportional counting region. Because of the high voltages (1350 to 1450 V) required in this counting mode, a quench gas (in this case, methane) must be present in the gas stream to reduce the large dead time of the counter.

The methane concentration necessary to maintain system stability and counting reproducibility is dependent on the applied voltage as well as on the level of expected counting. In preliminary experiments, an external source of radium-226 was used to demonstrate changes in counting efficiency while setting the electronic variables. A flowing gas mixture of known tritium concentration was then used to optimize counting conditions.

Table IV-4 presents the results obtained with two "homemade" ionization chambers of 25 and 240 ml nominal volume for a mixture of tritium and hydrogen in argon. Also given in the table is a value obtained by internal proportional counting for a sample of the same mixture. Although the data so far are limited, indications are that the counting efficiency is close to the expected value of 100% and that linearity of response is independent of a given chamber volume.

The effects on counting of changes in hydrogen and methane concentrations in the gas stream were tested. Hydrogen was of interest because it will be present at concentrations possibly as high as 1% in the gas stream to the ionization chamber. At potentials below 2300 V, no interferences were observed at hydrogen levels as high as 1.66%. At higher voltages and greater hydrogen concentrattions, preliminary results indicate somewhat

TABLE IV-4. Effect of Counting-Chamber Volume on Counting Efficiency for Tritium

Mixture used: argon containing ∿0.5 μCi T/liter and 40 ppm H_2

	Total cps	Bkg. cps	Net cps	Net cps/ml
25-ml counting chamber[a]	736	4.2	732	29.3
240-ml counting chamber[a]	7206	9.3	7197	30.0
I.P.C.[b] (5.25 ml)	-	-	141	26.8

[a]Conditions: methane composition, 3.25%; applied voltage, 2200 V (25 ml) and 2000 V (240 ml); flow rate through ionization chamber, 42.2 ml/min; single channel analyzer, integration mode.

[b]Internal proportional counting, Chemistry Division, ANL.

elevated count rates. Methane concentrations of less than ∿3% produced a sharp increase in count rate due to a decrease in the quenching action.

Ionization chambers having volumes of 20 and 85 ml are available commercially, and one of each of these sizes has been ordered. Although no significant difference is expected, the operating characteristics of each tube will be determined. The feasibility of operating the two tubes in series or parallel also will be explored. This method of operation should extend the flexibility of the tritium monitor if both the equilibrium and dynamic modes are used. It is expected that greater sensitivity (with a corresponding longer residence time and a slower response time) will be obtained using the larger counter.

A gas mixture containing a higher concentration of tritium and a more sensitive electronic flowmeter have been ordered. These items will be used to determine the linearity of the counting system at higher tritium concentrations and at lower flow rates.

V. SODIUM CHEMISTRY
(F. A. Cafasso)

A. Vacuum Distillation as a Method for the Analysis of Impurities in Sodium (R. A. Blomquist)

Vacuum distillation of a sodium sample followed by analysis of the residue is commonly used as a method for determining trace metals and selected nonmetals, including oxygen, in sodium. Many impurities can be determined in the residue by means of a specific analysis for the constituent of interest; however, oxygen is determined indirectly by analyzing the residue for sodium by titrimetry or atomic absorption and calculating the oxygen content on the assumption that the residue consists only of sodium oxide. Obviously, the presence in the residue of sodium-bearing species other than oxygen will result in an error unless appropriate corrections are made. The primary objectives of this work are to (a) determine which of the impurities that are likely to exist in sodium will be found as sodium-bearing species in the residue and hence introduce an error in the oxygen analysis and (b) find methods of avoiding the problem or, alternatively, gaining the capability for correcting the error introduced by the presence of other sodium-bearing impurities. A secondary objective is to investigate the potential of distillation as a general method for the anaysis of nonmetallic impurities in sodium. Work addressed to these objectives is described below.

The behavior of cyanide, a potential impurity in sodium systems, has been studied under distillation conditions. Sodium cyanide (~320 μg) was added to about 800 g of multiply distilled sodium in a nickel cup contained in a distillation apparatus. (The still and distillation procedure were described in ANL-7846, p. 46.) After distillation of the sodium at ~350°C, the residue was collected and analyzed for cyanide. About 50% of the added cyanide was found. This finding indicated that the presence of cyanide in sodium samples analyzed for "oxygen" will require analysis of the residue for cyanide and application of an appropriate correction.

The potential of the distillation method for the analysis of sulfur in sodium has also been explored. A sulfur method with a detection limit of 10 ppm is needed to determine whether purchased reactor-grade sodium meets the sulfur-impurity limit specified in RDT M 13-1T, Rev. 1, "Reactor Grade Sodium--Purchase Specifications."[1] Available sulfur methods do not possess the requisite sensitivity. To test the distillation method, approximately 9.8 mg of sulfur was added to ~800 g of sodium and a distillation conducted in a nickel cup. Analyses showed that only ~52% of the added sulfur was found in the residue. In a second experiment, in which 5.54 mg of sulfur was added to ~800 g of sodium, only ~67% of the added sulfur was recovered in the residue. To check the possibility that the sulfur may have been lost by reaction with the nickel cup, tests were also done in tantalum and titanium cups. The findings in these tests were similar to those of the first two tests. Therefore, it was concluded that the distillation approach was not a fruitful one for the analysis of sulfur in sodium.

---

[1]The maximum impurity limit for sulfur is 10 ppm.

B. Studies of Oxygen-Hydrogen Interactions in Sodium: Exchange Studies (A. K. Fischer)

This program has been concerned with the behavior of hydroxide in liquid sodium under conditions relevant to reactor operations. Two questions have been addressed: (1) Does hydroxide exist as a species in sodium under reactor conditions and if so, what is its stability? (2) If it is demonstrated to be unstable, what are the kinetics of its decomposition? Experiments to answer both these questions are virtually complete.

Previous experiments, in which deuteroxide was used as a stand-in for hydroxide, have shown that hydroxide exhibits metastability under the conditions of interest (ANL-7944, pp. 41-44). Recent work has been concerned with the reversal by hydrogen of the hydroxide decomposition reaction in liquid sodium and the determination of the kinetics of decomposition of a mixture of hydride and hydroxide at 500°C. A final statement of results of the current work will be presented when analysis of the data is completed.

VI. MATERIALS-COOLANT INTERACTIONS AND MECHANICAL-PROPERTY EVALUATIONS
(T. F. Kassner, R. W. Weeks)

The objective of this program is to provide a sound technical basis for determining the effect of the LMFBR sodium environment on the performance of fuel cladding, core structure, and out-of-core components. The required technology will be established according to the following plan: (1) determine the integrated effects of fast-neutron and sodium environments on the properties of stainless steel, (2) correlate mechanical-property and corrosion data obtained in reactor (EBR-II) and experimental sodium systems, (3) establish specifications for test specimens for sodium environmental tests, (4) develop postexposure testing methods and demonstrate their validity by correlation with in-sodium test data, and (5) develop a sufficient understanding of nonmetallic element transfer to predict compositional changes of materials in reactor sodium systems and ultimately relate these changes to the mechanical properties.

A. Development of Test-Specimen Characterization Methods and Procedures
(J. Y. N. Wang, J. J. Weins)

Methods are under development for the characterization of mechanical-property and corrosion specimens prior to and after exposure to high-temperature sodium in loop systems and in EBR-II for both in-core and out-of-core conditions. For interpretation and correlation of the mechanical-property data, the chemical composition and composition gradients in materials exposed to high-temperature sodium for long periods of time must be determined, as well as the amount, distribution, morphology and composition of the various phases that form as a result of thermal aging in a reactor environment. An early objective of this work is to define the extent to which various specimen-characterization methods must be employed and the usefulness of the information in establishing quantitative relationships between microstructural results and mechanical-property data.

An investigation of phase instabilities in Types 316 and 304 stainless steels as a function of time, temperature, degree of cold work, and carbon and nitrogen content of the materials is in progress to obtain a direct knowledge of the capabilities of the various specimen-characterization methods and to provide base-line microstructural information on thermal aging effects in the materials used in this program. Material from a small heat exchanger constructed from Type 304 stainless steel is also being examined to obtain additional information on the microstructural and compositional changes that occur after ∿8 yr of operation in low-velocity sodium at high temperatures. The details of the operating conditions of the heat exchanger were given in the previous quarterly report (ANL-7944, pp. 46-49), along with a schematic diagram and the microstructures of the material at various temperatures and locations.[1]

Additional information has been obtained on the heat-exchanger material as to the nonmetallic element composition, the type of phases present, their

---

[1]The schematic diagram and microstructures were given in ANL-7944, Fig. V-2, p. 48. Through an error in makeup, the figure was incomplete. The corrected figure is given at the end of this report.

relative amounts, and the microhardness. The carbon- and nitrogen-concentration gradients in the stainless steel, in the vicinity of the sodium-steel interface, were determined from analyses of 5-mil-thick sections machined from the material. The concentrations of these elements in the alloy were determined by combustion-manometric and wet chemical methods. The results, presented in Table VI-1, indicate that the stainless steel lost carbon at ∿700°C, whereas carburization of the surface regions occurred at lower temperatures. The nitrogen content of the alloy near the sodium-steel interface was lower than that in the bulk material at all temperatures between ∿700 and 450°C, although the extent of denitridation was small at the lower temperatures.

TABLE VI-1. Carbon and Nitrogen Analysis of Type 304 Stainless Steel Heat-Exchanger Material after ∿8 yr of Operation in a Low-Velocity Sodium Loop

Distance from Sodium-Steel Interface, mils	Carbon Conc., ppm, at Indicated Temp.			Nitrogen Conc., ppm, at Indicated Temp.		
	∿700°C	∿600°C	∿450°C	∿700°C	∿600°C	∿450°C
0-5	322	532	776	72	216	441
5-10	330	426	480	188	396	465
____[a]	402	428	449	452	452	472

[a]Center of 62-mil-wall, 0.5-in.-OD tube.

Scanning electron microscopy was used to identify precipitated particles in the material by spot analyses with an energy dispersive X-ray detector. The characteristic Kα peaks of Cr, Fe, and Ni indicated that the majority of the particles were the $M_{23}C_6$ carbide, although some sigma phase was present. The microhardness of the sigma phase was found to be five times greater than that of the austenite matrix.

For a quantitative determination of the amount of the phases present, specimens were anodically dissolved in 10% HCl-methanol solutions at low current densities. The weight fraction of the isolated residue was determined, and the residue was analyzed by an X-ray diffractometry technique with Cu-Kα radiation. The experimental "d" spacings and relative intensities are compared in Table VI-2 with ASTM standard values for the $M_{23}C_6$ carbide and the sigma phase. From an analysis of the areas under the characteristic peaks in the X-ray diffraction pattern, the residue was found to contain 93% $M_{23}C_6$ carbide and 7% sigma phase. On the basis of the total amount of residue collected, the absolute amounts of the carbide and sigma phase in the material at ∿700°C were 1.95% and 0.14%, respectively. The carbide content of the alloy determined by this method is in reasonable agreement with the total carbon

TABLE VI-2. Comparison of X-ray Diffractometry Results with ASTM Standard Values

ASTM Standard "d" Spacings[a]		Experimental "d" Spacings for Phases in the Residue[a]	
ASTM 14-407 $Cr_{23}C_6$	ASTM 5-0708 Sigma Phase	$Cr_{23}C_6$	Sigma Phase
2.37 (50)		2.37 (25)	
2.17 (50)		2.17 (30)	
	2.128 (100)		2.13 (60)
2.05 (100)		2.05 (100)	
	2.063 (80)		2.06 (30)
	2.015 (60)		2.02 (50)
	1.964 (80)		1.96 (50)
	1.923 (100)		1.92 (100)
	1.877 (80)		1.88[b]
1.88 (50)		1.88 (25)	
1.80 (50)		1.80 (20)	
1.78 (40)		1.79 (20)	
1.33 (40)		1.33 (5)	
1.29 (60)		1.29 (10)	
1.26 (100)		1.26 (10)	
1.23 (90)		1.23 (10)	

[a]Numbers in parentheses represent relative intensities (I/I_o).

[b]Superimposed line.

concentration of the sample determined by the combustion method.

The experimental procedure and methods of analysis that are being developed for correlating the composition and thermal history of austenitic stainless steels with the microstructures will be further used in the characterization of specimens prior to and after mechanical testing in a high-temperature sodium environment.

B. Development of Specimen-Exposure Facilities and Postexposure Mechanical-Property Testing Capability (J. J. Weins, R. W. Weeks)

The objective of this work is to develop the capability for (1) exposure of standard uniaxial and biaxial test specimens to sodium of controlled nonmetallic-element concentrations and (2) performing the postexposure property measurements in accordance with test conditions that provide design verification and operational support data to the FFTF. The information will also be compared with property data obtained in flowing sodium to establish the equivalence of in-sodium versus postexposure test results for alloys of the same composition and thermal history.

Five Satec uniaxial creep machines, shown in Fig. VI-1, are now operational in either an air or vacuum environment. Tests are being

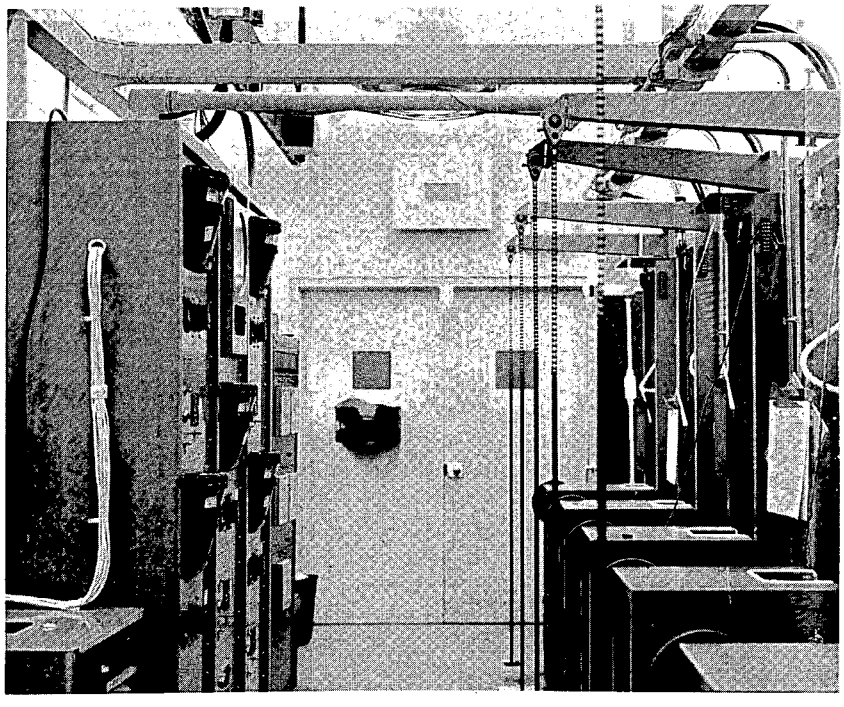

Fig. VI-1. Uniaxial Creep-Rupture Machines for Testing of Materials in Air, Vacuum, and Inert-Gas Environments after Exposure to Flowing Sodium. Neg. No. MSD-57645.

conducted in vacuum on Type 316 stainless steel specimens fabricated from heat V87210 for comparison with reported creep data on this material to evaluate the performance of these testing machines. An argon gas system has been designed for this equipment so that creep tests can also be performed in an inert-gas environment.

Four additional creep machines with Satec and Marshall furnaces, shown in Figs. VI-2 and VI-3, have been installed and are presently being used for testing in an air environment. These systems will also be modified for use in vacuum.

Uniaxial creep and biaxial tube specimens have been prepared for exposure to high-velocity, high-temperature sodium. These specimens will be included in a test section used for the exposure of FTR fuel-cladding material to sodium at a velocity of 20 ft/sec and a temperature above 700°C.

C. Studies of Carbon Transfer in Sodium-Steel Systems (K. Natesan, R. B. Snyder, T. F. Kassner, and C. A. Youngdahl)

A mathematical model is required to predict the magnitude and rate of carbon migration in FFTF and LMFBR systems under conditions in which temperature gradients and materials of different composition are present. These effects can then be related to mechanical-property changes in the materials. Several types of information are needed to formulate a model that is capable of describing the time-dependent carburization and/or decarburization of materials at various temperatures in a sodium system in which the sodium purity (e.g., carbon concentration) is also a variable. This information falls into three general categories: (1) materials data, (2) sodium-purity data, and (3) sodium-system parameters. The materials data include alloy composition, the activity and solubility of carbon in the alloy, metal-metal carbide phase-equilibria relations, volume and grain-boundary diffusion coefficients for carbon, and the thermal-mechanical history that influences the microstructure. The sodium-purity data primarily involve the carbon activity and solubility as a function of temperature. System parameters are the surface area of the material exposed to flowing sodium at different temperatures in the loop, the volume of sodium in the system, the presence of carbon sources and/or sinks in the system other than the primary construction materials, and operating conditions that may result in a large variation in the above parameters.

The relevant materials data for austenitic stainless steels, based upon experimental and calculated results, have been reported in previous quarterly reports (ANL-7868, pp. 53-56 and ANL-7944, pp. 50-60). This information is now being used in the formulation of kinetic rate equations for the carburization and decarburization of austenitic stainless steels in liquid sodium. The mathematical solution to these equations yields carbon concentration-penetration profiles in the stainless steels as a function of time, temperature, and surface carbon concentration in the material, the latter of which is established by the carbon concentration in sodium via the distribution coefficient. Depending upon whether the carbon activity produced by a given carbon concentration in sodium is greater or less than that in the alloy at any temperature, carburization

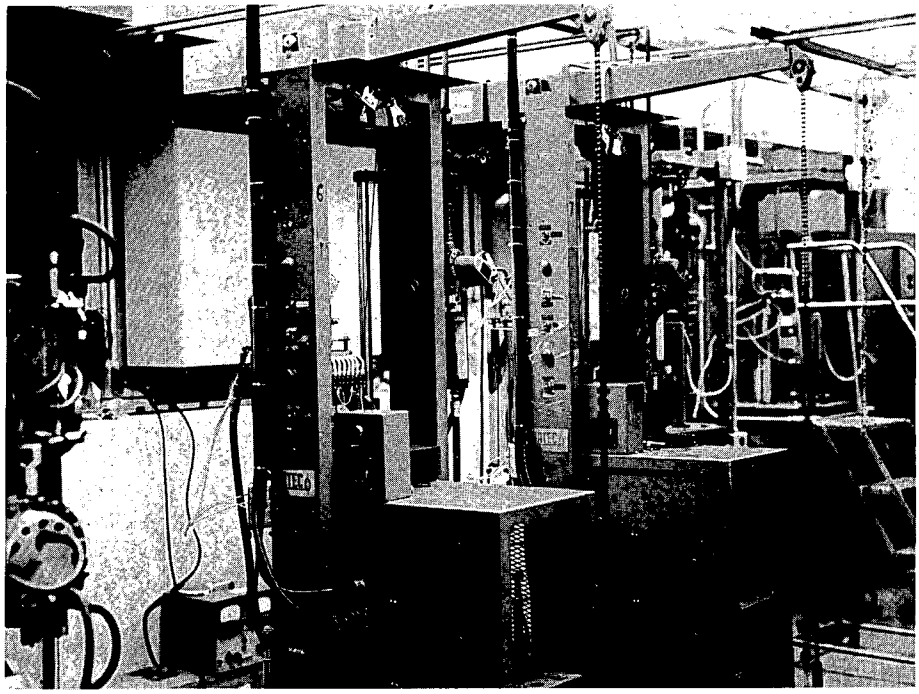

Fig. VI-2. Uniaxial Creep-Rupture Machines for Testing of Control Specimens in an Air or Vacuum Environment. Neg. No. MSD-57644.

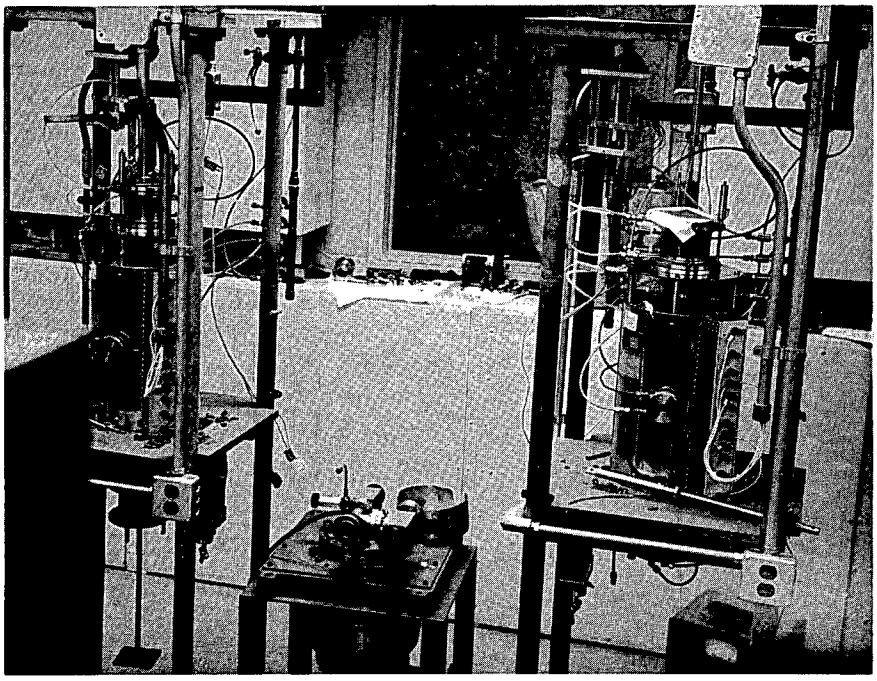

Fig. VI-3. Uniaxial Creep-Rupture Systems under Modification for Use in a Vacuum Environment. Neg. No. MSD-57646.

or decarburization will occur. The actual carbon concentration in the sodium is determined by the rate at which carbon is introduced into and removed from the sodium by the loop materials and by other sources or sinks that may be present in the system. For example, operating procedures such as the periodic insertion or removal of test specimens or hardware through a cover gas can dislodge "frost" containing sodium carbonate and other carbon-bearing species into the sodium. This material, upon dissolution, can increase both the oxygen and carbon concentrations of the sodium. Other circumstances and changes in operating conditions can also alter the carbon concentration in the sodium, since there is no provision for carbon control that is analogous to the cold trap for maintaining the oxygen and hydrogen concentrations of the sodium within a narrow range of values. To a large extent, these circumstances account for the wide range of carbon levels that have been observed in reactor materials upon exposure to high-temperature flowing sodium. Since reactor operations and operating conditions influence the carbon concentration in sodium, it is difficult to predict probable values with the degree of certainty required to relate this information to microstructural changes and the mechanical behavior of materials in the absence of a direct knowledge of the sodium purity (i.e., carbon concentration determined by a foil equilibration method rather than sodium sampling and analyses).[2]

The model that is being developed for carbon migration in sodium systems will accommodate the essential information on materials and system scaling factors to enable one to calculate compositional changes in the materials for a wide range of carbon concentrations in sodium where variations with time due to operating conditions can also be included. These results will be used to compare component performance, in terms of materials behavior, with design limits over the service life.

1. Development of Carbon-Diffusion Relations

The first step in the development of such a model is the formulation of rate equations for the carburization and decarburization of austenitic stainless steels. The process involves the diffusion of carbon accompanied by the precipitation or dissolution, respectively, of the $(Cr,Fe)_{23}C_6$ carbide in the austenite matrix. The carburization process is somewhat analogous to the internal oxidation of a reactive metal in a noble-metal matrix, which has been the subject of experimental and theoretical investigation.[3-9] The major difference between the two processes is that all of

---

[2]K. Natesan and T. F. Kassner, "Monitoring and Measurement of Carbon Activities in Sodium Systems," Submitted for publication in Nuclear Technology.

[3]F. N. Rhines, W. A. Johnson, and W. A. Anderson, Trans. Met. Soc. AIME, 147, 205 (1942).

[4]L. S. Darken, Trans. Met. Soc. AIME 150, 159 (1942).

[5]C. Wagner, Z. Elektrochem. 63, 772 (1959).

[6]J. H. Swisher and E. O. Fuchs, Trans. Met. Soc. AIME 245, 1789 (1969).

[7]R. A. Rapp, Corrosion 21, 382 (1965).

[8]D. E. Thomas, Trans. Met. Soc. AIME 191, 926 (1951).

[9]C. Wagner, Corrosion Science 8, 889 (1968).

the reactive metal in a noble-metal matrix is converted to oxide, whereas only a fraction of the chromium present in the steel reacts to form carbide during carburization and this amount increases with increasing carbon potential of the sodium. A direct application of the internal-oxidation rate equations to the carburization process without incorporating these modifications would grossly underestimate the thickness and overestimate the carbide volume fraction and total carbon content of the precipitated zone for any reaction time.

The mathematical formalism for internal oxidation was therefore modified to represent the carburization process more closely; however, the diffusion equations became more complex and a closed-form analytical solution could not be obtained even for simple boundary and initial conditions. Therefore, a numerical solution to the problem was obtained using a computer.

For one-dimensional diffusion of carbon accompanied by carbide precipitation, Fick's second law for the diffusion of carbon and chromium can be written as

$$\frac{\partial (N_C + \nu N_{CrC_\nu})}{\partial t} = D_C \frac{\partial^2 N_C}{\partial X^2} \tag{1}$$

$$\frac{\partial (N_{Cr} + N_{CrC_\nu})}{\partial t} = D_{Cr} \frac{\partial^2 N_{Cr}}{\partial X^2} \tag{2}$$

where

N_C, N_{Cr} = the mole fractions of carbon and chromium in the austenite phase, respectively;
N_{CrC_ν} = the number of moles of precipitated carbide per mole of the alloy;
ν = the atom ratio of carbon to chromium in the carbide, i.e., 6/23 for the $Cr_{23}C_6$ carbide;
D_C, D_{Cr} = the diffusion coefficients for carbon and chromium, respectively, in the austenite matrix;
X = the distance from the alloy surface; and
t = time.

When carbon and chromium in austenite form the $(Cr,Fe)_{23}C_6$ mixed carbide by the reaction

$$Cr_{(\gamma)} + \frac{6}{23} C_{(\gamma)} = \frac{1}{23} Cr_{23}C_6 \text{ (in mixed carbide)},$$

the relationship between the chromium and carbon concentrations in austenite in equilibrium with the carbide can be expressed as

$$N_{Cr} = A - B \ln N_C \tag{3}$$

where A and B are constants that were evaluated from carbon activity-concentration data for Fe-Cr-8 wt % Ni alloys at various temperatures.

With the use of Eq. 3 and the substitution of the variable $\eta = X/(4D_C t)^{1/2}$, the partial differential equations (Eq. 2 and 3) can be converted into the ordinary differential equation

$$-\frac{B}{N_C}\cdot\frac{dN_C}{d\eta}-\frac{1}{\nu}\cdot\frac{dN_C}{d\eta}=\frac{B}{2\eta}\cdot\frac{D_{Cr}}{D_C}\cdot\frac{d^2(\ln N_C)}{d\eta^2}+\frac{1}{2\nu\eta}\cdot\frac{d^2N_C}{d\eta^2} \qquad (4)$$

This equation was solved numerically by Hamming's modified predictor-corrector method[10] for N_C in terms of η for a fixed initial carbon concentration in the steel, e.g., 0.05 wt %, and for various surface carbon concentrations. The reaction zone was considered to be thin in relation to the thickness of the material, i.e., semi-infinite boundary. It was found that Eq. 4 could be simplified to the following form

$$\frac{d^2N_C}{d\eta^2}+\frac{2B\nu\eta}{N_C}\cdot\frac{dN_C}{d\eta}=0 \qquad (5)$$

without affecting the results. The contribution of two of the terms of Eq. 4 is negligible because the diffusion coefficient for chromium is several orders of magnitude smaller than that for carbon and, in the austenite phase, the time variation of the chromium concentration is much larger than that for carbon at any distance, X (i.e., $dN_{Cr}/d\eta \gg dN_C/d\eta$).

The total carbon concentration in the steel (carbon in the austenite plus carbon in the $M_{23}C_6$ carbide) was obtained as a function of position, for any time, by using calculated and experimental relationships between N_C and total carbon content of the alloy. The latter information was given in previous quarterly reports (ANL-7868, pp. 53-68 and ANL-7944, pp. 50-60). The above analysis is applicable to the carburization and decarburization of an austenitic stainless steel in which the initial and surface carbon concentrations exceed the solubility limit. Under decarburizing conditions in a sodium environment, the surface carbon concentration in the alloy can fall below the solubility value. Carbon diffusion through the single-phase austenite can be described by established solutions to Fick's second law:

$$N_C = N_C^s + (N_C^o - N_C^s)\ \mathrm{erf}\ \eta \qquad (6)$$

where N_C^s is the mole fraction of carbon in austenite at the sodium-steel interface and N_C^o is an iterative constant.[11] The incorporation of Eqs. 5

[10] IBM System/360 Scientific Subroutine Package, Version III, p. 337 (1970).

[11] In a single-phase material, N_C^o in Eq. 6 is the initial concentration of the solute element diffusing out of the alloy. During decarburization of an austenitic stainless steel, the composition of the austenite (e.g., carbon and chromium concentrations) changes in the two-phase (austenite + carbide) region in the vicinity of γ/γ + carbide interface. For this situation, a nonphysical value for N_C^o allows the carbon concentration, N_C, and the flux, $D_C \cdot \partial N_C/\partial X$, at the γ/γ + carbide interface obtained from Eq. 6, for the single-phase region, and that from Eq. 5, for the two-phase region, to attain the same respective values in order to fulfill the requirement for a singular carbon activity at the interface.

and 6 into the computer program along with the coupling condition at the γ/γ + carbide interface made it possible to generate carbon concentration-distance profiles for both carburizing and decarburizing situations.

2. Thermodynamic and Kinetic Input Parameters

The applicable thermodynamic and kinetic data in the diffusion relations are those that express the driving force for carbon migration in the material in terms of the carbon activity differences and the tracer or self-diffusion coefficient in austenite, rather than changes in the total carbon concentration and the apparent or effective diffusion coefficient. Both types of information can be used to generate carbon-diffusion profiles in austenitic stainless steels: the former approach is applicable to a wide range of temperatures and carbon levels in the materials, whereas the latter is restricted to specific conditions because of limited data for the dependence of the effective diffusion coefficient on both temperature and carbon level in the steel.

The data used in our analysis include the self-diffusion coefficient for carbon in Type 304 stainless steel from the work of Agarwala et al.[12] and carbon solubility and activity-concentration relationships obtained from the graphical data in Figs. V-1, V-3, and V-10 of ANL-7868. In addition to the carbon activity data, which were extrapolated from high-temperature results, an analytical expression was developed from the experimental data on the variation of the carbon activity with carbon concentration and temperature shown in Fig. VI-4. The temperature dependence of the solubility of carbon in sodium from the work of Longson and Thorley[13] (Fig. V-6 of ANL-7868) was used for the purpose of describing carburization-decarburization profiles of Type 304 stainless steel in terms of various carbon concentration levels in sodium.

3. Carburization-Decarburization Profiles for Type 304 Stainless Steel in Sodium

The carburization-decarburization behavior of Type 304 stainless steel was analyzed, in terms of the variables time, temperature, and carbon concentration in sodium, by incorporating the thermodynamic data extrapolated from high temperatures into the computer solution of the diffusion equations. The effect of time on the carbon-concentration profiles in the material at 700°C for 0.08 ppm carbon in sodium is shown in Fig. VI-5. Figure VI-6 shows the influence of the carbon content of the sodium in the range from 0.01 to 0.08 ppm on the surface carbon concentration and the carbon profiles in the material for 1 yr at 700°C. Depending upon the carbon concentration in sodium, carburization or decarburization of the material can occur. The effect of temperature on carbon profiles in the steel at 1 and 10 yr is shown in Figs. VI-7 and VI-8, respectively, for 0.01 ppm carbon in sodium. In these figures, the variation with temperature of the carbon concentration at the surface of the steel is shown in the plane corresponding to zero penetration in the material. The cross-over

---

[12] R. P. Agarwala, M. C. Naik, M. S. Anand, and A. R. Paul, J. Nucl. Mater. 36, 41 (1970).

[13] B. Longson and A. W. Thorley, J. Appl. Chem. 20, 372 (1970).

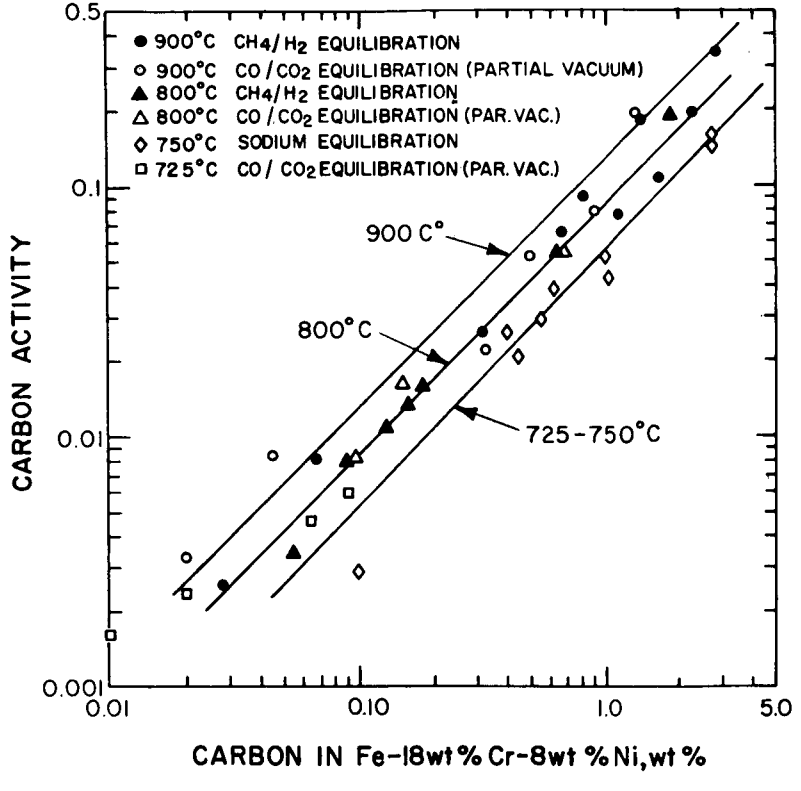

Fig. VI-4. Variation of Carbon Activity with Carbon Concentration in Fe-18 wt % Cr-8 wt % Ni Alloy at 725-750, 800, and 900°C by Equilibration in CO/CO_2 and CH_4/H_2 Gas Mixtures, and in Liquid Sodium. Neg. No. MSD-57470

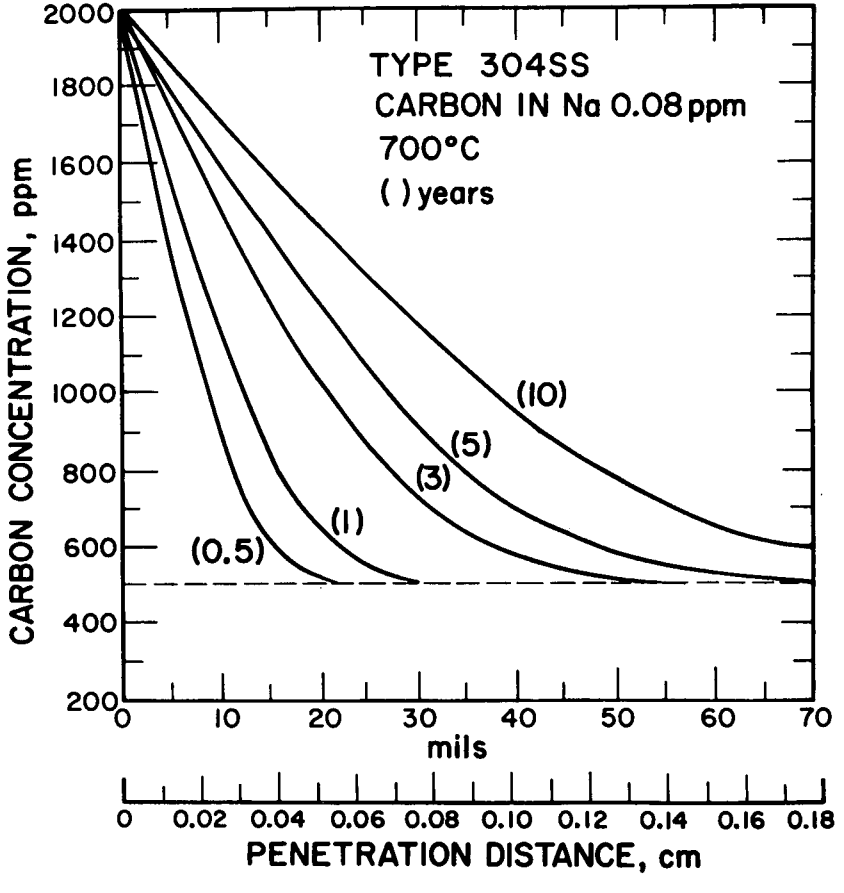

Fig VI-5. Effect of Time on Carburization Profiles for Type 304 Stainless Steel at 700°C and 0.08 ppm Carbon in Sodium, Based on Carbon Activity-Concentration Relationship Extrapolated from High-Temperature Data. Neg. No. MSD-57616

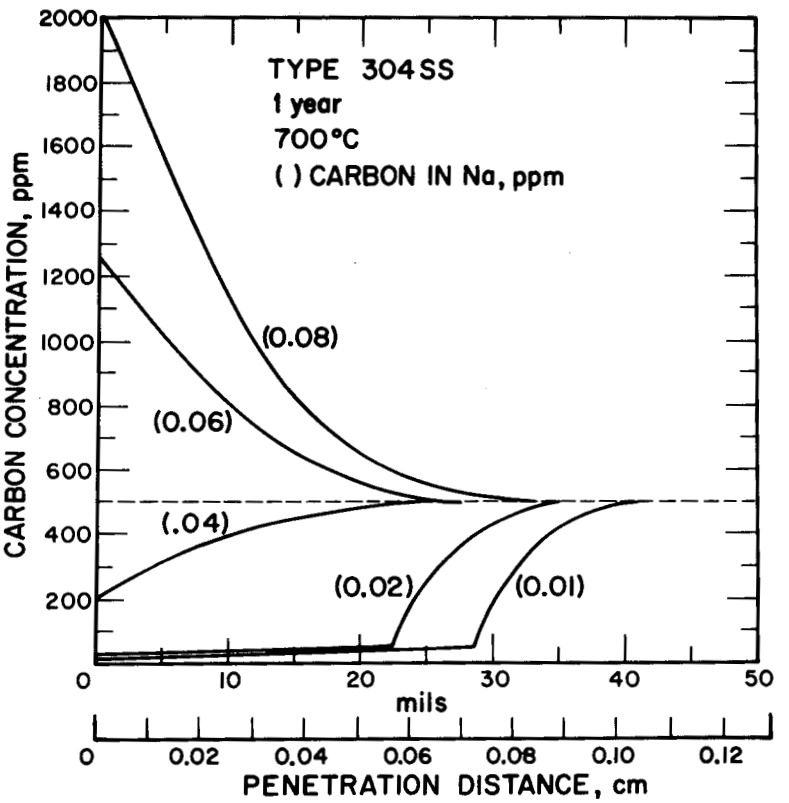

Fig. VI-6. Carburization and Decarburization Profiles in Type 304 Stainless Steel after 1 yr at 700°C for Various Carbon Levels in Sodium, Based on Carbon Activity-Concentration Relationship Extrapolated from High-Temperature Data. Neg. No. MSD-57611

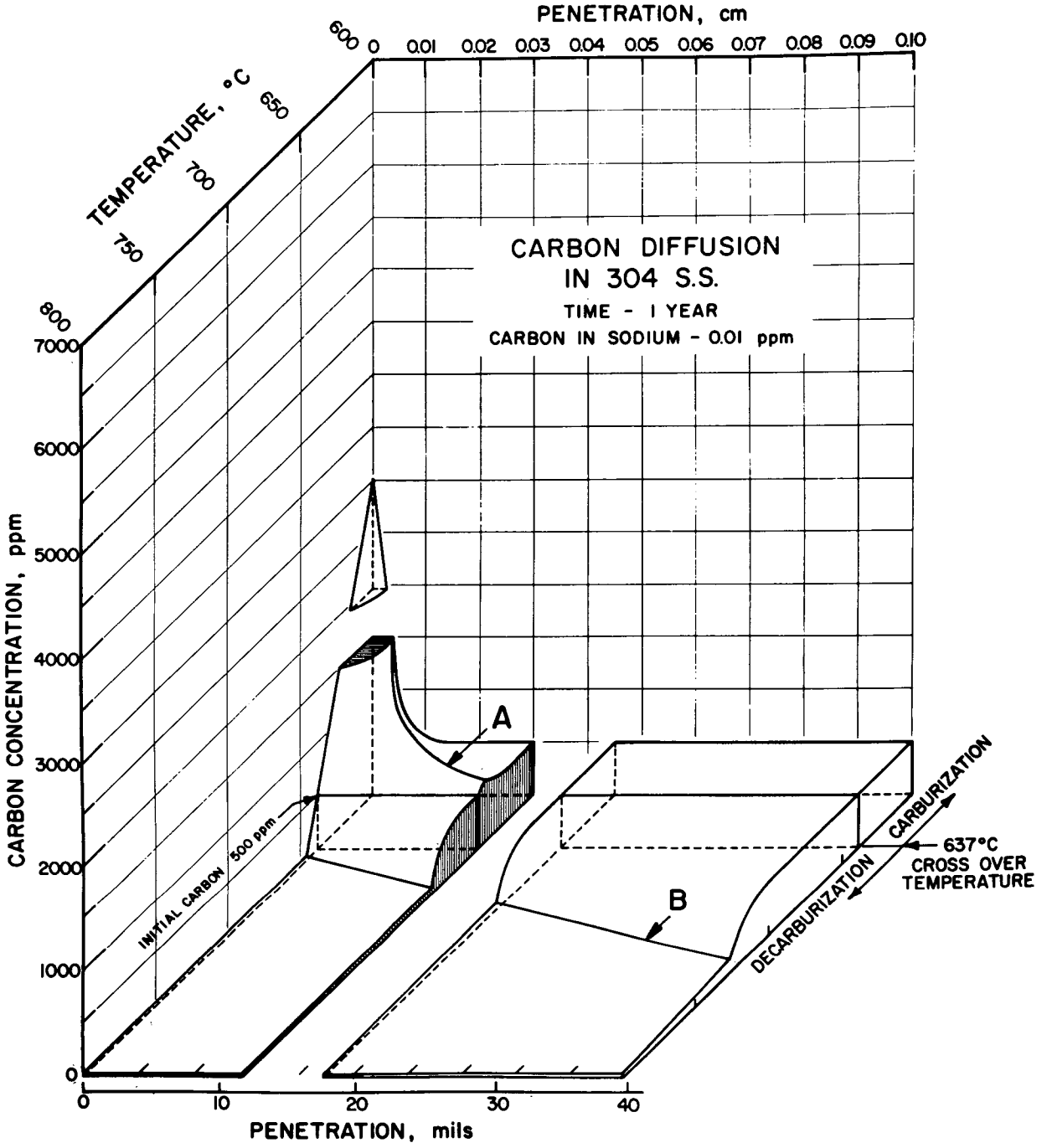

Fig. VI-7. Effect of Temperature on Carburization-Decarburization Behavior of Type 304 Stainless Steel Exposed for 1 yr to Sodium Containing 0.01 ppm Carbon, Based on Carbon Activity-Concentration Relationship Extrapolated from High-Temperature Data. Neg. No. MSD-57618

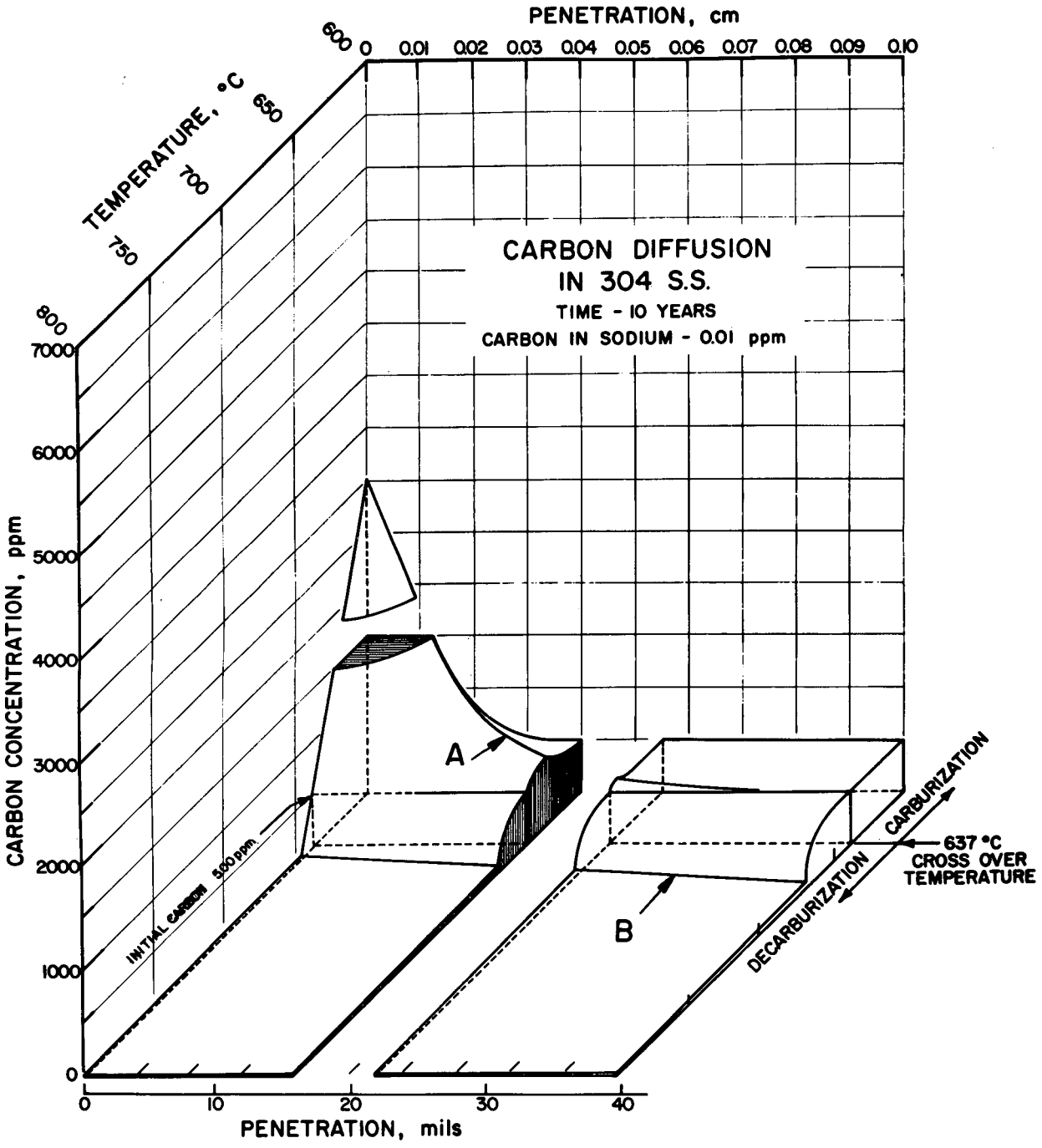

Fig. VI-8. Effect of Temperature on Carburization-Decarburization Behavior of Type 304 Stainless Steel Exposed for 10 yr to Sodium Containing 0.01 ppm Carbon, Based on Carbon Activity-Concentration Relationship Extrapolated from High-Temperature Data. Neg. No. MSD-57623

temperature between carburization and decarburization is 637°C for a steel with an initial carbon content of 500 ppm. Line A indicates the temperature variation of the region of maximum carburization. Line B represents the temperature variation of the penetration depth for the transition between the single-phase austenite and the two-phase austenite plus carbide mixture. The major effect of increasing the time from 1 to 10 yr in Figs. VI-7 and VI-8 is the increase in the depth of decarburization at temperature above the crossover value. The results of similar calculations for 0.08 ppm carbon in sodium and diffusion periods of 1 and 10 yr are shown in Figs. VI-9 and VI-10, respectively. Increasing the carbon concentration from 0.01 to 0.08 ppm increases the surface carbon concentration in the material and moves the crossover temperature to a higher value, both of which contribute to the greater degree of carburization.

The manner in which the carburization-decarburization behavior of Type 304 stainless steel is influenced by incorporating the experimental carbon activity-concentration data in Fig. VI-4 into the computer solution of the diffusion equations has also been determined. At low carbon activities, the measured carbon concentrations in the austenitic steel are much lower than those obtained by extrapolation of the higher temperature data to temperatures in the range from 600 to 800°C. Representative carbon concentration-distance profiles at 650°C as a function of the exposure time and carbon concentration in sodium are shown in Figs. VI-11 and VI-12, respectively. To illustrate both carburization and decarburization profiles in Fig. VI-12, a temperature below 700°C was required and, thus, a direct comparison of the profiles in Figs. VI-11 and VI-12 with those in Figs. VI-5 and VI-6 cannot be made from these figures. A plot analogous to Fig. VI-7, for carbon diffusion in Type 304 stainless steel for 1 yr and 0.01 ppm carbon in sodium, which is based upon the experimental carbon activity-concentration data in Fig. VI-4, is shown in Fig. VI-13. Only decarburization is predicted in the latter figure since the crossover temperature has decreased to 575°C. An increase in the exposure time from 1 to 10 yr would result in decarburization to a greater depth at any temperature; therefore, a plot similar to Fig. VI-8 was not made.

The effect of temperature on the carbon profiles at 1 and 10 yr for 0.08 ppm carbon in sodium, based on experimental carbon activity-concentration data, is shown in Figs. VI-14 and VI-15, respectively. A comparison of these results with the information in Figs. VI-9 and VI-10, which is based on extrapolated high-temperature data, indicates the following: (1) The surface carbon concentration in the steel is a factor of 2 to 5 times lower, depending upon the temperature. (2) The crossover temperature decreases from 725 to 685°C. (3) The decarburization behavior is not vastly different at higher temperatures (>750°C); however, the degree of carburization at the lower temperatures is considerably smaller.

Since the diffusion coefficient and solubility for carbon in the steel, as well as the carbon concentration and solubility in sodium, were not variables in the analysis, the differences in the two sets of results can be directly attributed to the carbon activity-concentration relationships that were used for the material. At the present time, we believe that the information in Figs. VI-11 to -15, based upon the experimental data in Fig. VI-4, represents a better approximation of the kinetics of carbon diffusion in the steel.

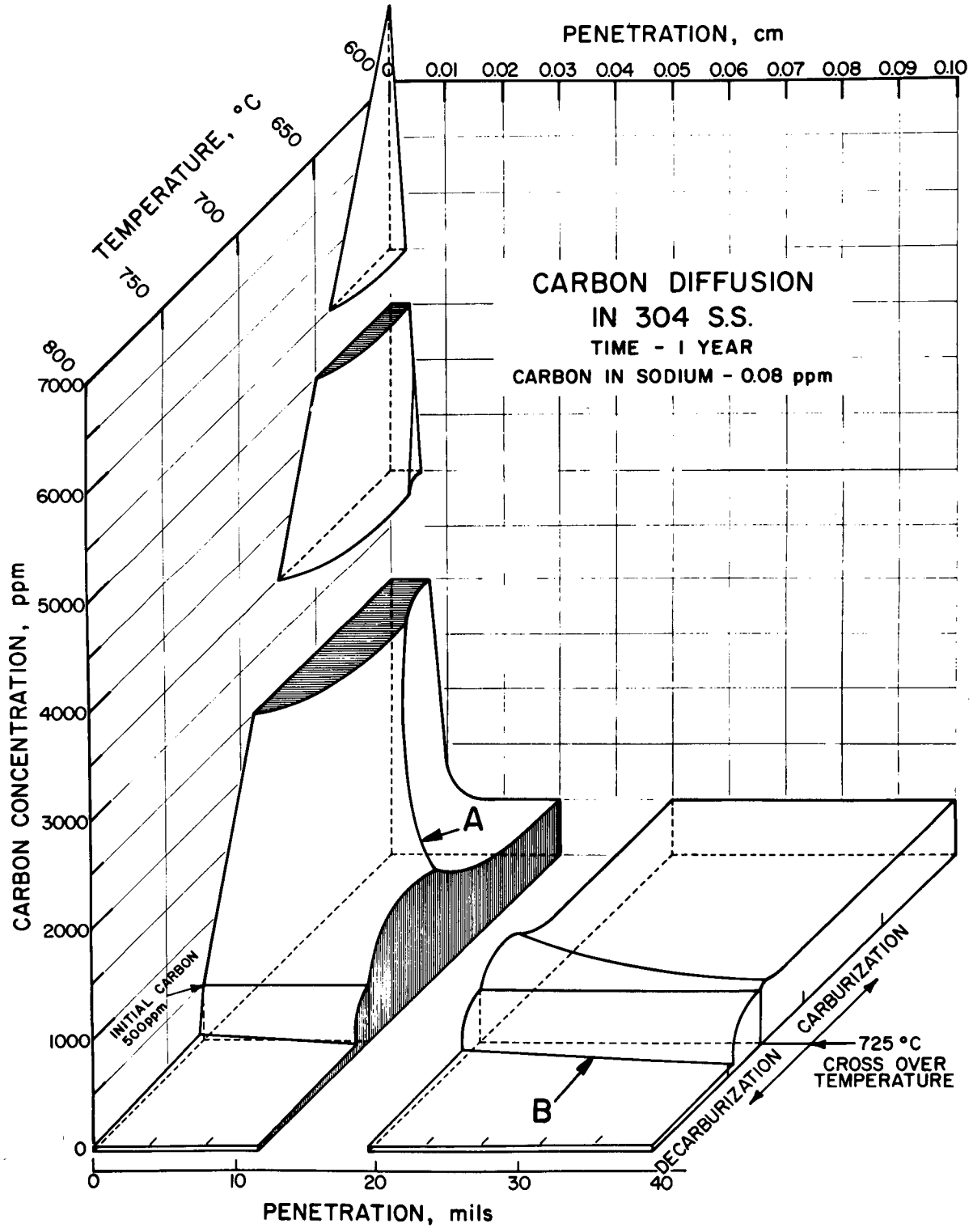

Fig. VI-9. Effect of Temperature on Carburization-Decarburization Behavior of Type 304 Stainless Steel Exposed for 1 yr to Sodium Containing 0.08 ppm Carbon, Based on Carbon Activity-Concentration Relationship Extrapolated from High-Temperature Data. Neg. No. MSD-57619.

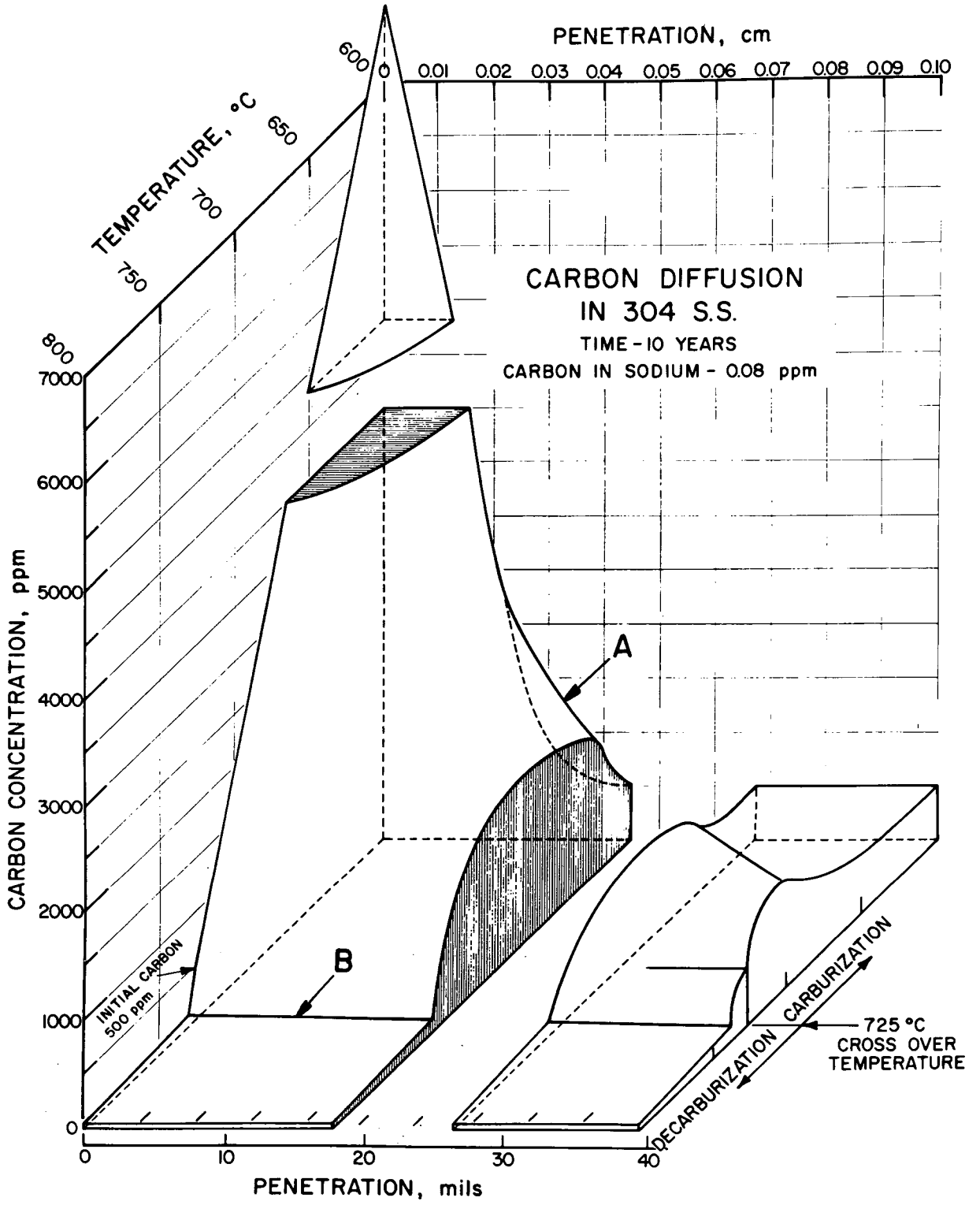

Fig. VI-10. Effect of Temperature on Carburization-Decarburization Behavior of Type 304 Stainless Steel Exposed for 10 yr to Sodium Containing 0.08 ppm Carbon, Based on Carbon Activity-Concentration Relationship Extrapolated from High-Temperature Data. Neg. No. MSD-57622

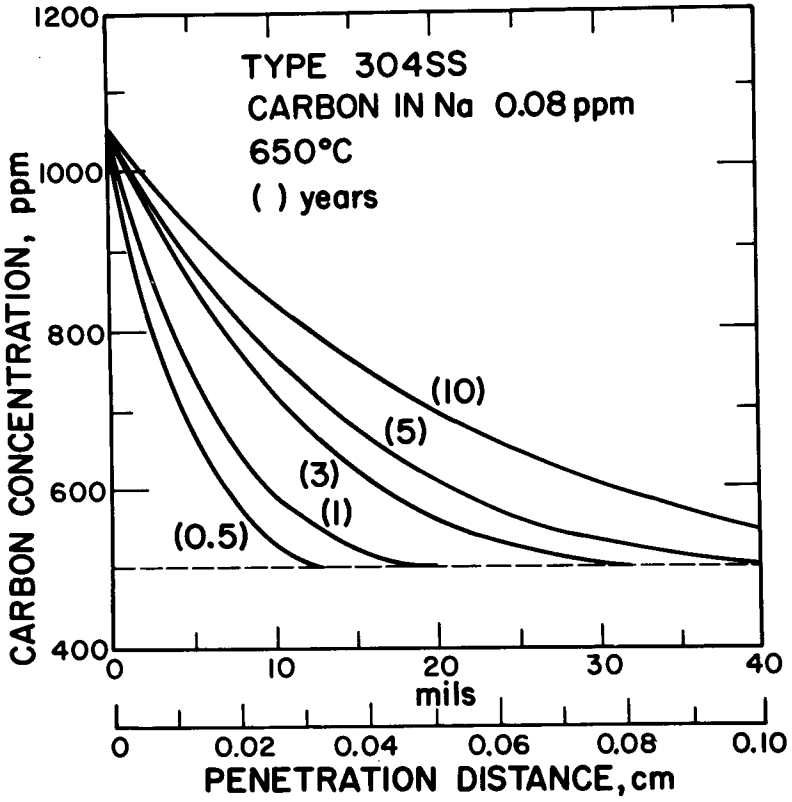

Fig. VI-11. Effect of Time on the Carburization Profiles for Type 304 Stainless Steel at 650°C and 0.08 ppm Carbon in Sodium, Based on Experimental Carbon Activity-Concentration Data. Neg. No. MSD-57615

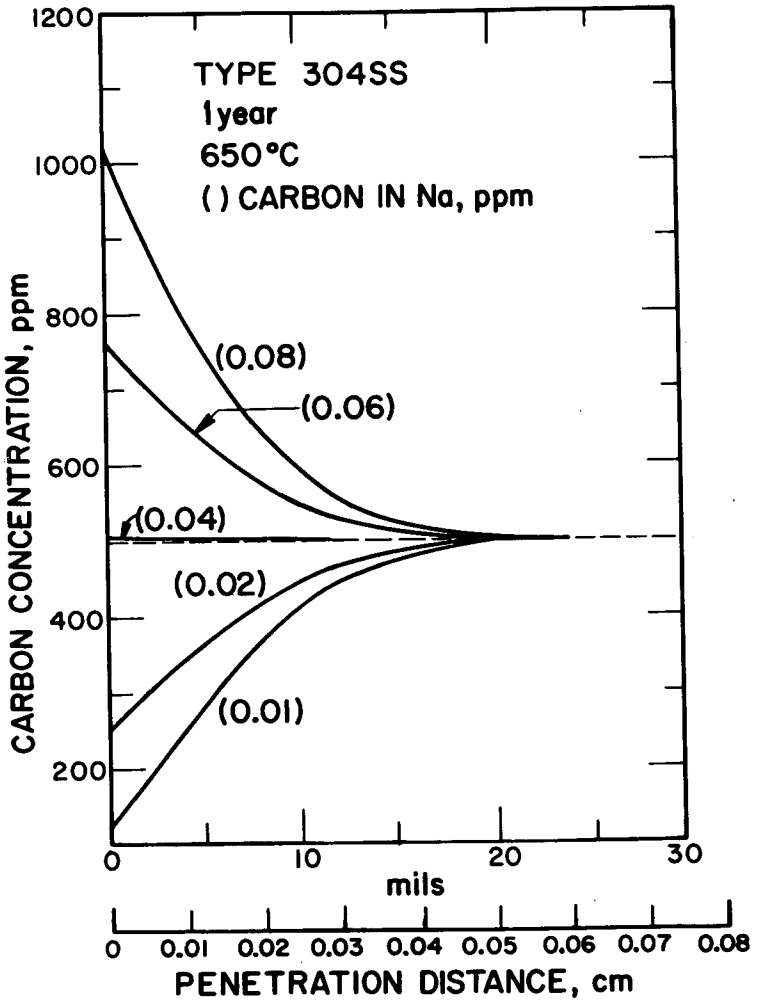

Fig. VI-12. Carburization and Decarburization Profiles in Type 304 Stainless Steel after 1 yr at 650°C for Various Carbon Levels in Sodium, Based on Experimental Carbon Activity-Concentration Data. Neg. No. MSD-57610

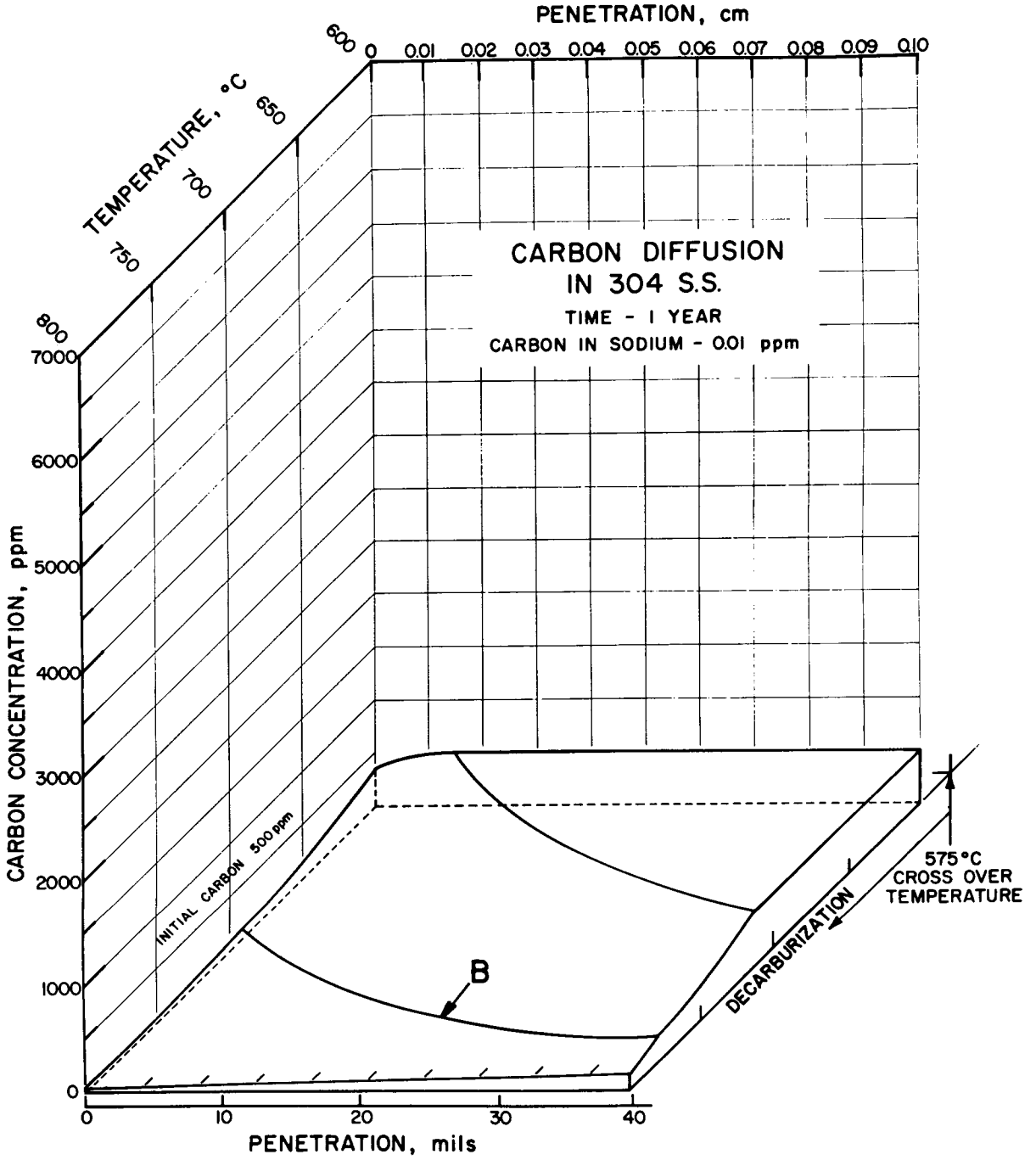

Fig. VI-13. Effect of Temperature on Decarburization Behavior of Type 304 Stainless Steel Exposed for 1 yr to Sodium Containing 0.01 ppm Carbon, Based on Experimental Carbon Activity-Concentration Data. Neg. No. MSD-57621

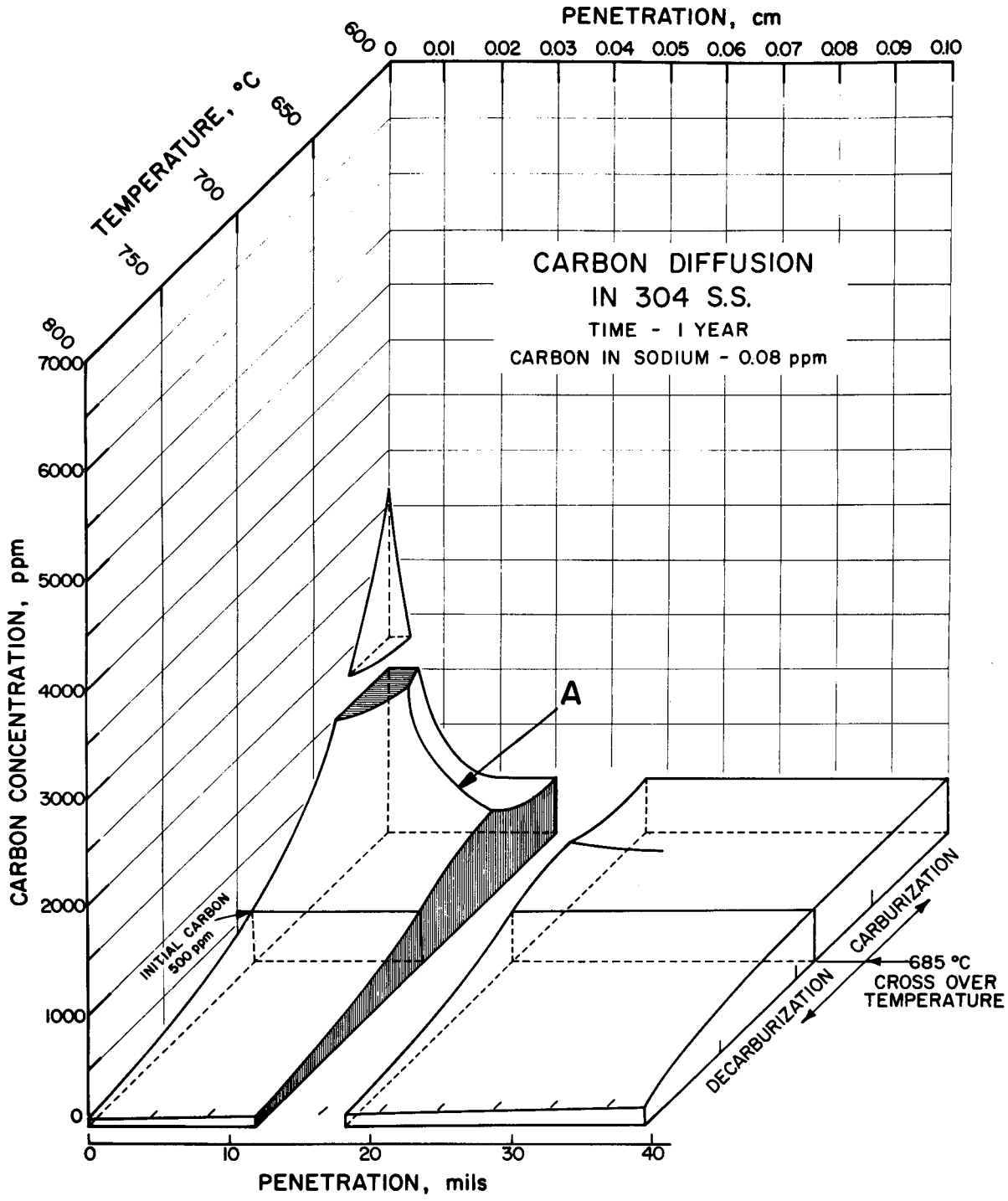

Fig. VI-14. Effect of Temperature on Carburization-Decarburization Behavior of Type 304 Stainless Steel Exposed for 1 yr to Sodium Containing 0.08 ppm Carbon, Based on Experimental Carbon Activity-Concentration Data. Neg. No. MSD-57617

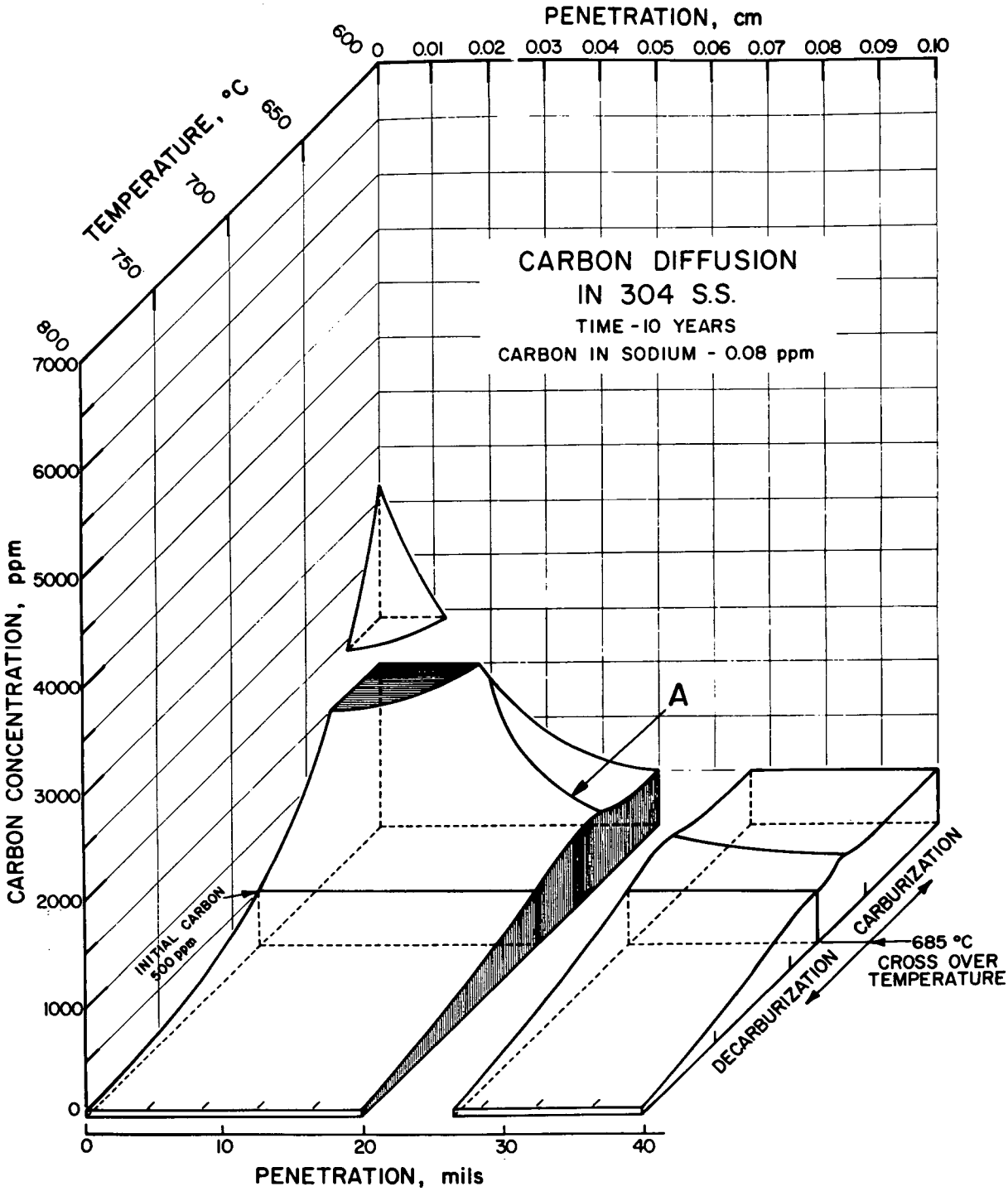

Fig. VI-15. Effect of Temperature on Carburization-Decarburization Behavior of Type 304 Stainless Steel Exposed for 10 yr to Sodium Containing 0.08 ppm Carbon, Based on Experimental Carbon Activity-Concentration Data. Neg. No. MSD-57620

The activity and diffusion data for the carbon that are being generated for various commercial austenitic stainless steels, along with a more accurate knowledge of the temperature dependence of the carbon solubility in sodium, will further increase the reliability of predictions on the carburization-decarburization behavior of these materials in a sodium environment. These predictions can then be compared with measured carbon-diffusion profiles in the materials at several exposure times, temperatures, and carbon levels in sodium to establish the validity of the results. The mathematical model will be extended to include conditions of nonuniform initial carbon distributions in the materials (commonly observed in tubing) and conditions in which the carbon concentration in sodium varies with time. Neither of these situations was considered in the preceding analysis, but may be required in the evaluation of carbon migration rates in experimental loops and reactor systems.

ERRATUM

ANL-7944

Sodium Technology Quarterly Report, January-March 1972

Figure V-2 in ANL-7944 (p. 48) was incomplete because of an error in makeup. The correct figure is given below.

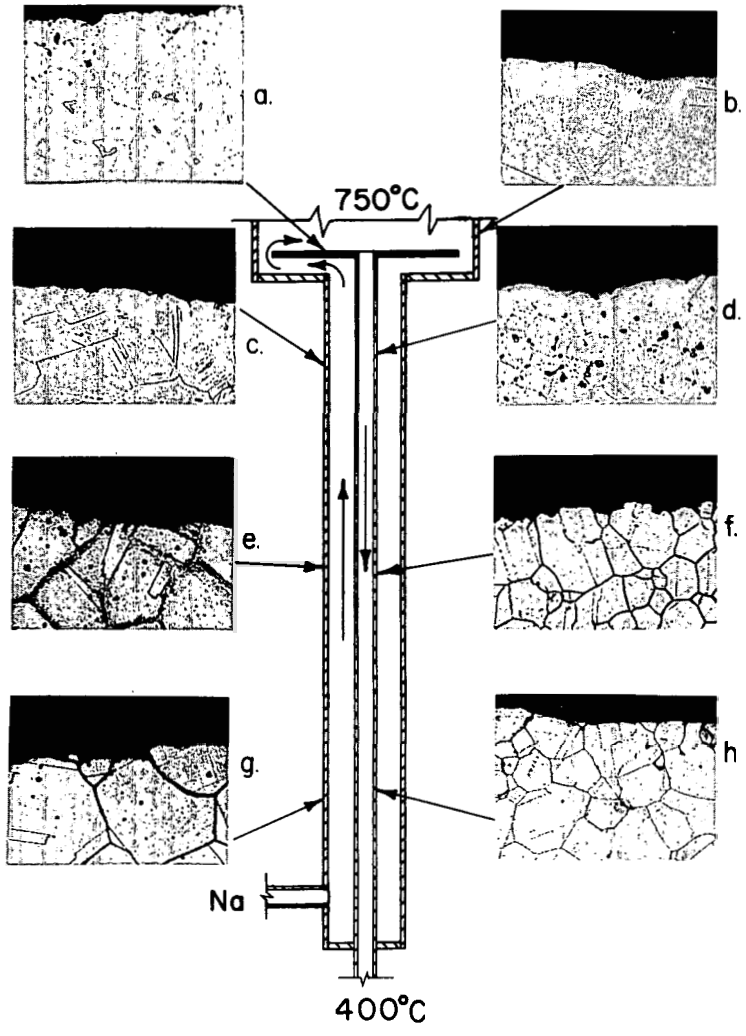

Fig. V-2. Microstructures of Type 304 Stainless Steel Heat-Exchanger Material after 8 yr of Exposure to Low-Velocity Sodium at Temperatures between 400 and 750°C ("a" Murakomi etched, all others electro-etched in 10% oxalic acid. Original magnification 350X). Neg. No. MSD-57133